

# TCBENCH: A BENCHMARK FOR TROPICAL CYCLONE TRACK AND INTENSITY FORECASTING AT THE GLOBAL SCALE

## Anonymous authors

Paper under double-blind review

## ABSTRACT

TCBench is a benchmark for evaluating global, short to medium-range (1-5 days) forecasts of tropical cyclone (TC) track and intensity. To allow a fair and model-agnostic comparison, TCBench builds on the IBTrACS observational dataset and formulates TC forecasting as predicting the time evolution of an existing tropical system conditioned on its initial position and intensity. TCBench includes state-of-the-art dynamical (TIGGE) and neural weather models (AIFS, Pangu-Weather, FourCastNet v2, GenCast). If not readily available, baseline tracks are consistently derived from model outputs using the TempestExtremes library. For evaluation, TCBench provides deterministic and probabilistic storm-following metrics. On 2023 test cases, neural weather models skillfully forecast TC tracks, while skillful intensity forecasts require additional steps such as post-processing. Designed for accessibility, TCBench helps AI practitioners tackle domain-relevant TC challenges and equips tropical meteorologists with data-driven tools and workflows to improve prediction and TC process understanding. By lowering barriers to reproducible, process-aware evaluation of extreme events, TCBench aims to democratize data-driven TC forecasting.

## 1 INTRODUCTION

Tropical cyclones (TCs), also called “hurricanes” or “typhoons” depending on the basin (American Meteorological Society, 2020), are globally devastating weather systems. In the U.S. alone, TCs caused over \$1.5 trillion in damages and over 7,000 deaths between 1980 and 2024 (NOAA National Centers for Environmental Information, 2025). With over half of the global population projected to live in the tropics and low-elevation coastal zones by 2050-2060 (Gu et al., 2021; Neumann et al., 2015), **improving TC forecasting is urgent** for risk mitigation and community resilience.

TC forecasting can be framed as the task of forecasting **two continuous time-series**:

**Track:** the time-series of storm locations in latitude  $\phi \in [-50, 50]^\circ$  and longitude  $\lambda \in [0, 360]^\circ$ ;

**Intensity:** commonly characterized by maximum sustained wind speed  $V_{\max} \in \mathbb{R}_+$  (m s<sup>-1</sup>) and minimum sea-level pressure  $p_{\min} \in \mathbb{R}_+$  (Pa). Both variables are used operationally.

Operational TC forecasts traditionally rely on physics-based models that solve coupled partial differential equations to simulate global weather fields, with nested higher-resolution grids in the vicinity of the TC (Hazelton et al., 2023). However, we require supercomputing infrastructure to run these models at a spatial resolution that marginally resolves TCs (Davis, 2018) and this limits their accessibility. This limitation, combined with the availability of high-quality, open-sourced benchmark datasets (Rasp et al., 2024), has led to an increased interest in data-driven weather forecasting (Ebert-Uphoff & Hilburn, 2023).

Several “neural weather models” now outperform state-of-the-art physics models on the 1–10 day forecasting of select meteorological fields at a  $0.25^\circ$  resolution (Rasp, 2024). Compared to physics-based models, neural weather models—once trained—are computationally efficient and help democratize forecasting. Neural weather models are scalable and ensemble well, which is a desirable property in large forecasts to quantify and reduce uncertainty. Nonetheless, the performance of neural weather models is often summarized in metrics calculated over the global prediction and [focus less](#) on

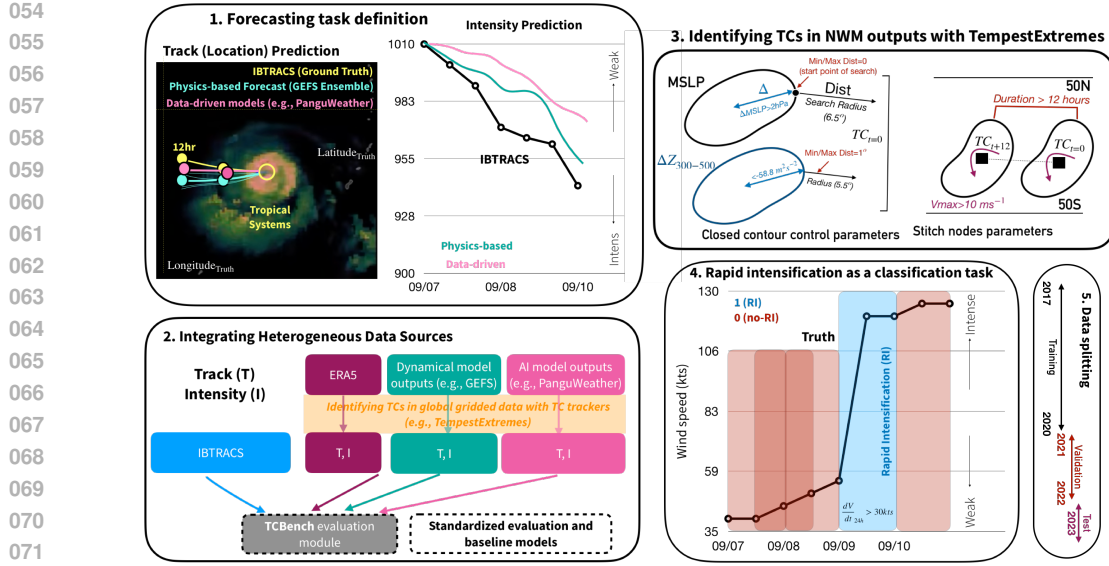


Figure 1: TCBench defines TC forecasting as predicting time-series of track and intensity knowing the system’s initial state. It integrates heterogeneous data sources (observations, reanalysis, physics/data-driven models) into a unified evaluation framework to standardize model assessment.

process-based assessments and divergent approaches in evaluation complicates comparison between models. For example, PanguWeather (Bi et al., 2023) and FourCastNet (Pathak et al., 2022) rely on author-defined TC tracking algorithms, GraphCast (Lam et al., 2023) optimizes tracking for each model, and GenCast (Price et al., 2025) relies on a well-established tracking algorithm (Ullrich et al., 2021) but is forced to adapt it due to the frequency of their model outputs. Furthermore, other data-driven approaches that focus on basin specific predictions (e.g., Huang et al., 2023; Park et al., 2023) provide specialized predictions that may outperform global approaches, given the variance in meteorological and oceanographic characteristics that drive TC behavior in each basin (Singh et al., 2025).

While TC track prediction from neural weather models now rivals (DeMaria et al., 2024) and sometimes outperforms physics-based models (Broad, 2024), TC intensity prediction remains a major challenge. We know that intensity change of TCs is primarily determined by the oceanic energy available for the TC to extract and the vertical structure of temperature in the vicinity of the TC (Emanuel, 1986). It is thus possible to derive the theoretical maximum energy achievable by a TC based on sea level pressure, sea surface temperature, relative humidity, and outflow layer temperature (MPI—maximum potential intensity; e.g., Emanuel, 1999). Furthermore, the main processes that keep TCs from intensifying and reaching their theoretical MPIs include vertical wind shear, which introduce dry air intrusion into the TC (Wong & Chan, 2004; Alland et al., 2021), and upwelling of cold deep ocean water underneath the TC (Price, 1981). Though some recent models explicitly predict an ocean variable (e.g., sea surface temperature Price et al., 2025), most predict strictly atmospheric data. Given that the state of the ocean can have a strong impact on TC intensity even under adverse atmospheric conditions (Nickerson et al., 2025), this is likely to present an additional challenge for accurately representing intensity. Furthermore, the spatial resolution of physics-based global models is often too coarse to represent anomalies in wind speed, wind extremes, in TCs (DeMaria et al., 2014; Baker et al., 2024). Similarly, neural models are often forecast low intensity due to biases in their training data (Dulac et al., 2024). As a result, current data-driven intensity forecasts frequently under-perform simple baselines such as persistence and climatology (DeMaria et al., 2024).

Accurate modeling of TC intensity is of special importance, given that Rapid Intensification (RI)—defined as a large increase in intensity over a short period of time, typically around the 95<sup>th</sup> percentile of intensification in a 24h window—is frequently observed in the most destructive TCs (Lockwood et al., 2024b; Knutson, 2024) and the frequency of such storms is projected to increase with anthropogenic warming Li et al. (2023). Furthermore, RI forecasting remains a major challenge because it arises from nonlinear interactions between environmental forcing and inner-core dynamics Wang

108 & Wu (2004). These multiscale processes involve inner-core features such as eyewall dynamics,  
 109 vortex Rossby waves, and rainband structures, along with external influences including vertical  
 110 wind shear and synoptic flow. The balance between these internal and external factors governs how  
 111 efficiently a storm can intensify, and their nonlinear coupling across scales makes RI particularly  
 112 difficult to predict. Yet, the predictive performance of neural weather models for RI has to our  
 113 knowledge rarely been systematically assessed in previous literature. In this work, we treat RI as a  
 114 **binary classification task**, which determines whether  $V_{\max}$  will increase by at least 30 kt ( $\approx 15.4 \text{ m}$   
 115  $\text{s}^{-1}$ ) over 24 hours (Kaplan & DeMaria, 2003; Kaplan et al., 2010), emphasizing that this roughly  
 116 corresponds to the 95th percentile of the rate of intensity increase. By formulating RI evaluation in  
 117 this way, we aim to evaluate how these models could be used as flags in warning systems. This is  
 118 important given the need for better forecasting of these events to coordinate prompt responses and  
 119 minimize the impacts associated with these storms (Appendini, 2024).

120 In this work, we present TCBench, a benchmark dataset that **bridges state-of-the-art neural and**  
 121 **physics-based weather models with TC observational records to accelerate progress in data-**  
 122 **driven forecasting of TCs**. This enables a transparent, reproducible assessment of how TC prediction  
 123 can be further improved with machine learning. We demonstrate that neural weather models can  
 124 skillfully forecast TC intensity up to 5 days ahead, particularly when combined with observational  
 125 data and processed through tools provided in TCBench. Furthermore, we show that ensemble neural  
 126 weather models demonstrate TC track prediction skill that rivals traditional, physics-based ensembles.

127 TCBench frames the problem of TC forecasting under the assumption that there is already a tropical  
 128 system that exists at an initial time of forecast, thereby focusing on predicting how the system will  
 129 evolve. TCBench provides pre-processing pipelines, evaluation protocols, visualization tools, and  
 130 baselines from both physics- and neural-based models to benefit the atmospheric science and AI  
 131 communities. Designed for rapid iteration and anticipating fast innovation in data-driven forecasting,  
 132 TCBench is extensible to new models, additional predictive targets, and encourages creative use of  
 133 the data's spatiotemporal structure.

## 2 RELATED WORK

134 **Statistical models skillfully forecast TC intensity up to 5 days ahead when combined with**  
 135 **physics-based global atmospheric models, a strategy known as “statistical-dynamical” predic-**  
 136 **tion.** A prominent example is the Statistical Hurricane Intensity Prediction Scheme (SHIPS, (DeMaria  
 137 & Kaplan, 1994; Kaplan & DeMaria, 1999; DeMaria et al., 2005)), which uses a multiple regression  
 138 model with area-averaged climatological, persistence, satellite observations, and environmental  
 139 predictors from physics-based models to forecast TC intensity. Statistical-dynamical TC intensity  
 140 prediction models remain in use operationally due to their skill, particularly at longer forecast lead  
 141 times (Cangialosi et al., 2020). Statistical-dynamical models are also skillful at predicting RI, unlike  
 142 purely physics-based models (Torn & DeMaria, 2021). Statistical-dynamical methods for RI forecasts,  
 143 such as the SHIPS Rapid Intensification Index, or SHIPS-RII (Kaplan et al., 2010; 2015), use linear  
 144 discriminant analysis (Kaplan et al., 2010; Knaff et al., 2018), Bayesian and logistic regression  
 145 models (Rozoff & Kossin, 2011; Knaff et al., 2018), binomial logistic regression (DeMaria et al.,  
 146 2021), as well as consensus models (Kaplan et al., 2015).

147 In recent years, **machine learning models have begun tackling the problem of TC intensity**  
 148 **prediction.** Machine learning models trained on SHIPS predictors and satellite imagery skillfully  
 149 predict TC intensity and RI (Su et al., 2020; Griffin et al., 2022), as well as intensity and track errors  
 150 (Barnes et al., 2023; Fernandez et al., 2025). Convolutional neural networks (CNNs) and k-means  
 151 clustering better distinguish between environments that are favorable and not favorable to RI (Mercer  
 152 et al., 2021). Other approaches, such as decision tree-based models trained on SHIPS predictors  
 153 (Shaiba & Hahsler, 2016), the random Forest-based RI Scheme (FRIA) (Slocum, 2021; Sampson  
 154 et al., 2023), and the Long Short-Term Memory method (Yang et al., 2020) have also shown skill in RI  
 155 prediction. The advent of neural weather models for the global atmosphere opens new opportunities  
 156 for data-driven post-processing, analogous to statistical-dynamical prediction, with the **potential to**  
 157 **significantly extend the lead time for skillful TC forecasts.**

158 TCBench targets the challenging problem of global TC forecasting, providing open,  
 159 real-time-available data for these notoriously difficult-to-predict phenomena in an accessible format  
 160 designed to accelerate improvement of data-driven models (Table 1). As key contributions from

162 TCBench to the community, we include routines to deterministically and probabilistically evaluate  
 163 tracks predicted by models, neural weather model output data associated with our selected test  
 164 year, and the necessary inputs for the training and validating postprocessing baselines—facilitating  
 165 evaluation by community members of their own models and approaches with respect to the provided  
 166 baselines. Furthermore, our forecasting setup provides a straightforward comparison between TC  
 167 track prediction models to our best observational record, and does not limit comparisons to storms  
 168 predicted by all models. Finally, we as provide scores for baseline models and thereby streamline  
 169 comparisons between current and future models.

170

171

172

173

174

175

176

177

178

179

180

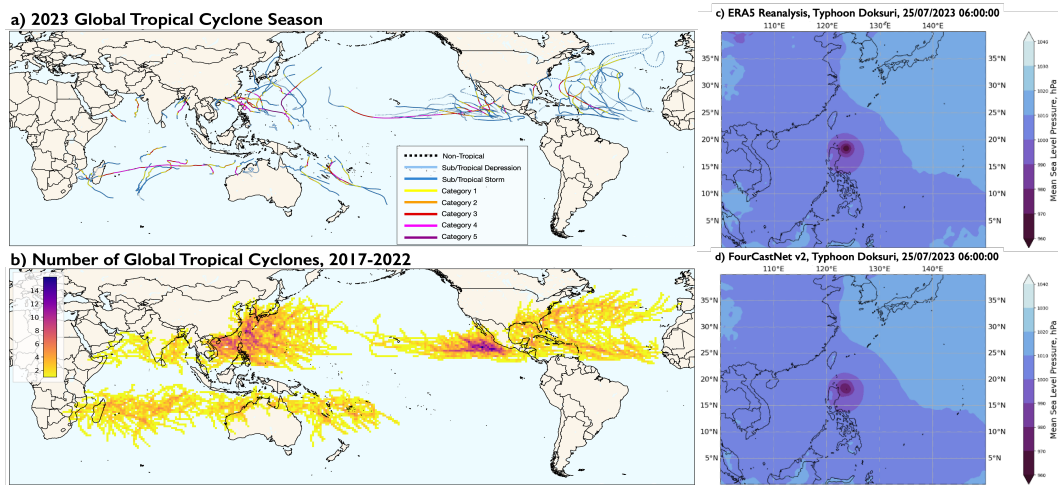
Dataset	Forecast evaluation	Global coverage	Open source	TC-specific	Environ. predictors	AI-ready format
WeatherBench <sup>2</sup>	✓	✓	✓	✗	✓	✓
ChaosBench <sup>2</sup>	✓	✓	✓	✗	✓	✓
SHIPS <sup>3</sup>	✗	✗	✗	✓	✓	✗
IBTrACS <sup>4</sup> (“ground truth”)	✗	✓	✓	✓	✗	✗
TC-PRIMED <sup>5</sup>	✗	✓	✓	✓	✓	✓
TropiCycloneNet <sup>6</sup>	✗	✓	✓	✓	✓	✓
<b>TCBench</b>	✓	✓	✓	✓	✓	✓

181 Table 1: Comparison of datasets and benchmarks across key criteria: forecast evaluation support,  
 182 coverage, openness, TC specificity, environmental predictors, and ML readiness.

183 <sup>1</sup> Rasp et al. (2024); <sup>2</sup> Nathaniel et al. (2024); <sup>3</sup> DeMaria et al. (2022); <sup>4</sup> Knapp et al. (2010); <sup>5</sup> Razin et al. (2023);

184 <sup>6</sup> Huang et al. (2025).

### 3 TCBENCH DATA TOOLBOX



205 Figure 2: **(a)** 2023 tropical cyclones in the TCBench test year, from IBTrACS. The lines represent  
 206 the position of each tropical cyclone over time, with the line color representing the storm’s intensity  
 207 at that position. **(b)** IBTrACS estimate of tropical cyclone numbers from 2017-2022 (corresponding  
 208 to TCBench’s training and validation years). Tropical cyclone counts binned into a  $1^{\circ}$  latitude  
 209 by  $1^{\circ}$  longitude grid. **(c)** Mean sea level pressure from ERA5 reanalysis during Typhoon Dokuri,  
 210 25/07/2023 06:00:00 UTC. Represents the ground truth targeted by neural weather models, as opposed  
 211 to the best record of TC intensity (IBTrACS) **(d)** 6-hour forecast of sea level pressure from the  
 212 FourCastNet-v2 neural weather model during Typhoon Dokuri, valid at 25/07/2023 06:00:00 UTC.  
 213 Panels a) and b) were made using the troPYcal software package (Burg & Lillo, 2019).

214 To provide a clear test set and baselines ensuring fair inter-model comparison, TCBench integrates a  
 215 diverse set of climate data with physics-based and neural weather model forecasts. A summary of

216 all data sources used in TCBench is provided in Appendix C. These sources were selected based  
 217 on availability, spatial resolution, historical record length, and their relevance to forecasting or post-  
 218 processing TC intensity of tracks (Section 3.2). Figure 2 provides an example of some of the various  
 219 data sources included in TCBench, including observed TC track and intensity data (Figure 2a,b),  
 220 reanalysis (Figure 2c), and neural weather model forecasts (Figure 2d). In addition to the data we  
 221 provide, we set forth guidelines for community members to submit data/and or models for their  
 222 evaluation and listing on the leaderboard.

### 224 3.1 DATA PROVIDED WITH TCBENCH

225 **The International Best Track Archive for Climate Stewardship (IBTrACS) serves as the “ground**  
 226 **truth” for model evaluation.** IBTrACS is the most complete observational archive of global TCs that  
 227 is currently available (Knapp et al., 2010; Gahtan et al., 2024). IBTrACS provides global coverage of  
 228 TC tracks, including various parameters, such as location, intensity, and size. For consistency, we  
 229 retain only the 6-hourly time stamps (00:00, 06:00, 12:00, 18:00 UTC). We note that the definition of  
 230 TC intensity is inconsistent across different meteorological agencies (Schreck III et al., 2014). In  
 231 TCBench, we use the U.S. agencies’ definition: minimum sea-level pressure and 1-minute maximum  
 232 sustained wind speed at an altitude of 10 meters, both of which are provided in IBTrACS. Another  
 233 source of uncertainty and inconsistency across agencies and time periods is the first data point  
 234 included in each TC track in the IBTrACS dataset, e.g. there is no specific intensity for when the  
 235 agencies start the track of a specific TC. We provide tools for processing the IBTrACS file provided  
 236 by NOAA and provide the subsection of data of interest per identified TC.

237 **ERA5** (Hersbach et al., 2020) is the 5th generation reanalysis product provided by the European  
 238 Centre for Medium-Range Weather Forecasts (ECMWF). ERA5 provides dozens of meteorological  
 239 variables at high spatial, vertical, and temporal resolutions, and models or assimilates a large amount  
 240 of historical data. Though ERA5 is used to provide initial conditions to physical and neural weather  
 241 models, we do not provide this data as it is made available by the ECMWF through its Copernicus  
 242 programme.

243 **Physics-based models** predict the weather by solving partial differential equations, such as the  
 244 laws of fluid dynamics, thermodynamics, radiative transfer, and atmospheric chemistry. We include  
 245 hindcasts from several of these models via The International Grand Global Ensemble (TIGGE)  
 246 product, including ensemble hindcasts of the Global Ensemble Forecasting System (the GEFS) and  
 247 the International Forecast System (the IFS)(Bougeault & Coauthors, 2010). In contrast, **neural**  
 248 **weather models** make weather forecasts using entirely data driven methods. These methods vary by  
 249 model but include graph neural networks (Lam et al., 2023), Fourier Neural Operators (Pathak et al.,  
 250 2022), and vision transformers (Bi et al., 2023). We include hindcasts from several neural weather  
 251 models, including NVIDIA’s FourCastNetv2 (Bonev et al., 2023), Huawei’s Pangu-Weather (Bi et al.,  
 252 2023), Google DeepMind’s GenCast (Price et al., 2025), and the ECMWF’s single-member AIFS  
 253 v1.0 (Lang et al., 2024).

254 With regards to **data processing**, all datasets were reformatted into a unified structure based on  
 255 IBTrACS for consistency across sources, using the IBTrACS storm identifier for identifying TCs and  
 256 following unit conventions in IBTrACS. For the physics based models, track data (position, intensity)  
 257 from international weather prediction centers was extracted from .xml files and standardized to  
 258 the format. For neural weather model forecasts, forecast tracks and intensities were parsed from  
 259 model outputs and matched to IBTrACS using TempestExtremes (Ullrich et al., 2021) and HuracanPy  
 260 (Bourdin & Saffin, 2025) and then standardized to the format. The postprocessing models we  
 261 provide predict intensification via a parametric distribution, and we thus sample in order to follow the  
 262 standardized. Additional details for the postprocessing models are provided in Appendix D.4.

### 263 3.2 DATA INCLUSION CRITERIA

264 To ensure consistency and usefulness across all experiments, each forecast or model dataset included  
 265 in TCBench had to meet the following requirements: a) They must provide at least 2 forecast  
 266 initializations per day (00z, 12z); b) They must provide forecasts at least through a 5-day lead time,  
 267 or forecasts until the IBTrACS record for that TC ends; c) the forecasts must be available as 6-hourly  
 268 forecast data; d) the forecasts must provide at least the latitude, longitude, minimum pressure, and  
 269 maximum wind speed track variables; e) models must provide any accompanying environmental

270 fields (e.g., surface wind speed, surface pressure, geopotential height; [additional examples are given](#)  
 271 [in Appendix C](#)) used for tracking and intensity estimation; f) if tracking storms in environmental  
 272 fields, a documented tracking algorithm and reproducible code examples; and g) if not directly  
 273 forecasting track and intensity, the provided fields must have a minimum resolution [corresponding to](#)  
 274 [about 0.5° on a global lat-lon grid](#), preferably 0.25°. These criteria are guidelines for both the data  
 275 we provide, and data provided by community members in the future.

276

### 277 3.3 GUIDELINES FOR MODEL SUBMISSION

278

279 **Dataset Split Recommendation:** IBTrACS storms are divided based on the year they occurred  
 280 to prevent leakage, noting that we divide based on calendar year and not TC season. We suggest at  
 281 least 4 years be used for training and at least 2 years be used for validation, noting that we assign  
 282 2017-2020 to training and 2021-2022 to validation. **We require that the year 2023 be left for**  
 283 **testing**, given that the models we include as baselines are not trained or tuned on this year.

284 **Model Submission Guidelines:** TCBench submissions must include: a) a list of open data sources  
 285 used for model training, including any relevant links; b) any additional data needed to run the model  
 286 on the test set; c) the minimal data sources needed to train the baselines presented for the training  
 287 and validation years, d) code and hyperparameters to train and run the model and generate the  
 288 predictions, e) the model and/or trained weights in a standard format (e.g., a pickled file – .pkl), f)  
 289 and an environment file to recreate the computing environment (or a container with which to run the  
 290 model). All data will be added to the GitHub and HuggingFace repositories as appropriate.

291

## 292 4 TCBENCH BENCHMARKING TOOLBOX

293

294 TCBench provides a standardized set of metrics to provide objective comparisons for TC forecasting.

295

296 **Intensity:** Intensity forecasts are evaluated using the root mean square error (RMSE) and the mean  
 297 absolute error (MAE).

298 **Track Error Metrics:** To evaluate the quality of predicted storm tracks, a set of deterministic  
 299 error metrics is computed following the methodology described by Heming (Heming, 2017). These  
 300 include:

302 **Direct Positional Error (DPE):** The straight-line distance between the forecast and observed  
 303 storm positions at the same verification time.

304 **Cross-Track Error (CTE):** The component of DPE that lies perpendicular to the observed storm  
 305 motion, indicating lateral displacement.

306 **Along-Track Error (ATE):** The component of DPE that lies along the observed storm motion,  
 307 indicating whether the forecast storm is ahead or behind in time.

308 A complete description of the formulae and computational procedures is provided in Appendix E.

309

310 **Probabilistic Evaluation:** To quantify uncertainty in ensemble forecasts, we report the fair variant  
 311 of the continuous ranked probability score (CRPS). Given an ensemble of  $N$  forecast values  $\{x_i\}_{i=1}^N$   
 312 and an observation  $y$ , the fair CRPS provides an unbiased estimation of the discrepancy between the  
 313 forecast distribution and the observed outcome:

$$314 \text{CRPS}(\{x_i\}, y) = \frac{1}{N} \sum_{i=1}^N |x_i - y| - \frac{1}{2N(N-1)} \sum_{i=1}^N \sum_{j=1}^N |x_i - x_j|. \quad (1)$$

315

316 The first term captures ensemble accuracy (mean absolute error), while the second reflects ensemble  
 317 sharpness (spread). Lower CRPS indicates better-calibrated forecasts centered on the observation.  
 318 We define **Track CRPS** for TC tracks by replacing absolute differences with Haversine distances  
 319 between predicted and observed storm center positions.

320 **Rapid Intensification Evaluation:** Though Rapid intensification (RI) is a rare event, it is not  
 321 exceedingly so. We define it as approximately the 95th percentile of intensity change over a 24-hour

Closed Contour Command Parameters				Stitch Nodes Parameters	
Variable	Delta	Dist. (°)	Min/Max Dist. (°)	Parameter	Value
MSLP	200 Pa	6.5	0	Minimum Track Duration	12h
$\Delta z_{300,500}$	$-58.8 \text{ m}^2 \text{s}^{-2}$	5.5	1.0	$V_{\max}$ Threshold	10 m/s
				Latitude ( $\phi$ )	$ \phi  \leq 50^\circ$

Table 2: TempestExtremes Parameters. Distances are expressed in great circle degrees.

window. Thus, we evaluate model performance on RI forecasts using metrics more tailored for rare event forecasts. We note that while most of TCBench is configured as a **regression** problem, we have formulated RI as a **binary classification problem**. Thus, rapid intensification models are tasked with making a simple “yes/no” prediction for the occurrence of rapid intensification (i.e., the presence of an intensification of 30 knots per 24h window, where the window is rolled over the 120h forecasts). For these metrics, TP refers to true positives (hits); TN refers to true negatives, or correct negatives; FP refers to false positives, or false alarms; and FN refers to false negatives, or misses.

**Critical Success Index (CSI):** Also known as the Threat Score, measures the ratio of correctly predicted positive observations to the sum of all predicted positives, actual positives, and minus true positives. CSI can be used both for probabilistic track evaluation and RI.

$$\text{CSI} = \frac{\text{TP}}{\text{TP} + \text{FN} + \text{FP}},$$

## 5 BASELINES

Following standard evaluation procedures (Knaff et al., 2003), we first compare TC forecasts to the Mean Tendency by Lead & Basin (MT-LB) and persistence baselines. MT-LB samples the empirical distribution of IBTrACS targets (intensity and position changes relative to initial conditions) from 1980 to 2022, conditioned on basin and lead time. For Persistence, at each lead time  $L$  the forecast equals the initial state at  $t_0$  (i.e., we predict neither motion nor a change in intensity)

**Baselines for Track and Intensity Predictions:** We provide scores for tracks obtained directly from DeepMind’s Weather Lab website for GenCast and Weatherlab FNV3, and for the ECMWF IFS ensemble and the NCEP GEFS models using tracks from the TIGGE dataset. For PanguWeather, FourcastNetv2, and the single-member version of AIFS, we process global outputs to obtain tracks using TempestExtremes (Ullrich et al., 2021). The parameters we used are listed in Table 2, and are the same as in Ullrich et al. (2021), with the exception of the minimum track duration, which is set to 12h. While this would normally lead to overly sensitive tracking (i.e., resulting in less filtering of short-lived systems that are not true cyclones), we frame the problem of TC prediction with the assumption that there is a prior system of interest known to exist at an initial time and we are interested in the evolution of said tropical system. We thus eliminate all spurious tracks that could not be matched to the systems of interest. We generate two sets of tracks to evaluate - one in which there is a fall back to the persistence baseline whenever the model does not produce a forecast for a storm (e.g., because the storm does not exist in the model outputs) and one that includes only the storms predicted by the models. Our main results rely on the former, while plots associated with the latter can be found in Appendix F.

We provide additional baselines that post-process data-driven weather model forecasts to predict tropical cyclone intensity, using a pipeline that follows (Gomez et al., 2025). These baselines provide only an intensity forecast, and a more thorough description of these baselines is given in Appendix D.4. Finally, we use all baselines for intensity prediction to evaluate for rapid intensification (RI) by thresholding the wind speed change—i.e., if the 24 hour change in wind speed is at least 30 kts, RI has occurred.

378 **6 RESULTS**  
 379

380  
 381 In this section we present examples of using TCBench to evaluate the deterministic and probabilistic  
 382 skills of neural weather models (AI Models) and physics-based models on TC track and intensity  
 383 predictions, covering lead times of up to five days. The results are summarized in Figures 3 and 4.

384  
 385 **Some AI Models perform well for tracks:** As shown in Figure 3, track prediction skills deteriorate  
 386 with increasing lead time. All evaluated models exhibit track errors that are smaller than the  
 387 persistence error at all lead times, indicating that all models produce useful track prediction. This is  
 388 especially apparent when looking at the error for the predicted tracks without a fallback to persistence,  
 389 shown by Figure 6 in Appendix F. While the track error for most AI models and physics-based  
 390 models are very similar across lead times, we see a clear indication of the AIFS model to outperform  
 391 other models in deterministic metrics beyond 24 hours. We largely attribute this to AIFS producing  
 392 TC track predictions for a greater number of time steps (see Figure 7 in Appendix F ), which  
 393 greatly reduces the number of samples for which the evaluation falls back to the persistence baseline.  
 394 Regarding the quality of model track ensembles, the physics-based GEFS model still outperforms the  
 395 AI model alternatives we evaluated with regards to track displacement CRPS. These results highlight  
 396 the potential of some existing data-driven forecasting models to provide **reliable deterministic** TC  
 397 track forecasts, but suggest that they are yet to be as good as physics-based ensemble models in  
 398 probabilistic track predictions.

399  
 400 **Postprocessing AI models yields skillful intensity predictions:** The coarse spatial resolution  
 401 of the physics-based global weather prediction models and the underlying training data for the AI  
 402 models mean that neither type of model is likely to perform well for intensity predictions. In fact,  
 403 all models produce forecasts of  $V_{\max}$  and  $p_{\min}$  that are worse than the persistence baseline for  
 404 shorter lead times but that outperform it for longer lead times (fig. 3). We see that the lead time at  
 405 which the intensity predictions become useful varies between 24 hours and 48 hours, and that the  
 406 physics-based GEFS model tends to perform best for both  $V_{\max}$  and  $p_{\min}$ . However, the difference in  
 407 deterministic and probabilistic skills between the best raw AI model and GEFS is slight. Furthermore,  
 408 we do not discount the possibility that a high spatial resolution, non-global physics-based model  
 409 can be dramatically better than both GEFS and the AI models at predicting TC intensity. Finally,  
 410 a well-designed post-processing algorithm of raw AI predictions can improve upon an originally  
 411 inaccurate AI model (e.g., PanguWeather) to the extent of producing predictions on par with or better  
 412 than the GEFS model.

413  
 414 **Only the postprocessed AI models capture RI:** The challenges of predicting TC RI events with  
 415 existing global AI models and physics-based models can clearly be observed in Fig. 4, where most  
 416 models show little to no ability to forecast such events across different lead times. Of the models we  
 417 evaluated, only the post-processed PanguWeather model shows any skill at RI prediction, with some  
 418 success in detecting RI for lead times between 48 and 96 hours. We note that neural weather models  
 419 have generally been trained on ERA5 reanalysis, which is known to have a negative bias with regards  
 420 to TC intensity. This issue, combined with the fact that many models have been trained to reduced a  
 421 mean error (e.g., MAE, RMSE) and the relatively coarse resolution of the predicted fields, makes  
 422 predictions of rapid intensification by the models a significantly more challenging task.

423 Overall, our evaluation reveals that:

- 424 • Some AI models outperform GEFS in deterministic track prediction, but not probabilistic ones.
- 425 • GEFS provides slightly better deterministic and probabilistic intensity forecasts than AI models.
- 426 • Intensity forecasts from AI models can be improved with a postprocessing pipeline.

427 These findings emphasize the complementary strengths of neural and physics-based systems, and  
 428 point toward hybrid approaches as a promising future direction in TC forecasting. These findings  
 429 also agree with (DeMaria et al., 2024; Sahu et al., 2025), who found that neural weather models  
 430 could make skillful TC track predictions, but lacked skill in intensity forecasting. The results from  
 431 the post-processed neural models are encouraging and point the way towards making data-driven TC  
 432 intensity forecasts more reliable.

## 432 7 DISCUSSION AND CONCLUSION

## 433

434 **Other Potential Applications:** In addition to the simple deterministic and probabilistic TC track  
435 and intensity predictions presented above, the TCBench dataset can be applied to other scientific  
436 applications related to different aspects of tropical cyclones. These include assessments of wind-  
437 related risks posed by tropical cyclones, tropical cyclone wind and precipitation nowcasting, wind  
438 field reconstruction, and data aggregation for physics discovery. Additional description of these  
439 potential applications is provided in Appendix G.

440 **Limitations:** There are clear limitations regarding this work, including the variance and evolution  
441 of uncertainty in the data, a limited selection of sources for tractability, and TC track inconsistencies  
442 across agencies. We acknowledge these and expand on them further in Appendix H.

443 **Conclusion:** By emphasizing flexibility in data experimentation, TCBench provides a data foundation  
444 that can be extended with advancements in TC observations and modeling. TCBench’s goal is  
445 to help the research community improve TC forecasts, our understanding of the physical processes  
446 governing TC behavior, ultimately mitigating TC impacts on local communities and society at large.  
447 We additionally provide a common point of comparison between TC forecasting models that is  
448 centered around the prediction of TC behavior once systems have formed. We show that for this task  
449 there is ample space for further research and improvement beyond our current data-driven forecasting  
450 capabilities, and provide tools for helping researchers in this field.

451

452

453

454

455

456

457

458

459

460

461

462

463

464

465

466

467

468

469

470

471

472

473

474

475

476

477

478

479

480

481

482

483

484

485

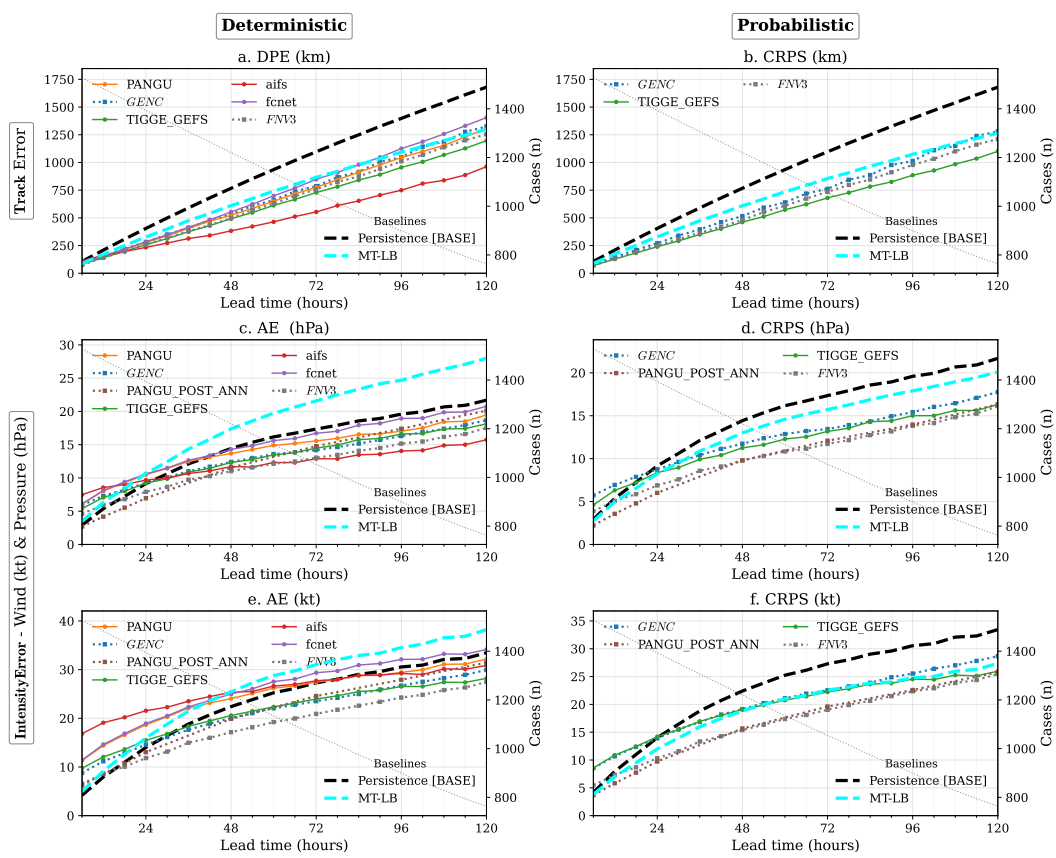


Figure 3: **FAIR per-lead comparison on TCBench-2023.** Deterministic (left) and probabilistic (right) scores from 6–120h for: **(a)** DPE, **(b)** CRPS–track, **(c)** AE–pressure, **(d)** CRPS–pressure, **(e)** AE–wind, **(f)** CRPS–wind. Means are computed on IBTrACS verification keys (00/12Z inits), with missing entries filled via persistence for fair comparison. Baselines: persistence (black dashed) and **MT-LB** (cyan dashed; mean tendency by lead & basin from IBTrACS, 1980–2022). For CRPS, persistence equals the MAE delta forecast. **GENC** and **FNV3** are italicized because we use the providers’ tracks (not re-derived). The post-processing model (dotted; e.g., **PANGU\_POST\_ANN**) deviates from our protocol (non-6 h lead grid; trained/validated on different years). Right axes show IBTrACS case counts. See SI for the corresponding raw (non-filled) comparison.

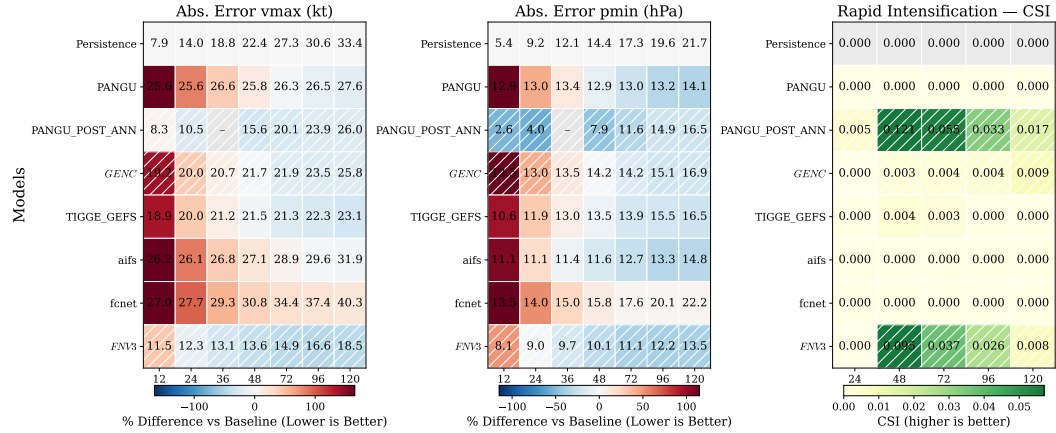


Figure 4: TCBench deterministic scorecard (2023, baseline = Persistence). Cells show mean error; colors show % difference vs baseline at the same lead (12–120h; columns) for each model (rows).

540 8 LLM USAGE DISCLAIMER  
541542 Conversational AI tools (e.g., ChatGPT and Copilot) were used for the following tasks during the  
543 manuscript's preparation: text editing (specifically, in making certain sections more succinct), latex  
544 formatting, and as an aid in code development when writing the benchmark framework.  
545546 REFERENCES  
547548 Shreya Agrawal, Luke Barrington, Carla Bromberg, John Burge, Cenk Gazen, and Jason Hickey.  
549 Machine learning for precipitation nowcasting from radar images. *arXiv preprint arXiv:1912.12132*,  
550 2019.551 Ferran Alet, Ilan Price, Andrew El-Kadi, Dominic Masters, Stratis Markou, Tom R Andersson,  
552 Jacklynn Stott, Remi Lam, Matthew Willson, Alvaro Sanchez-Gonzalez, et al. Skillful joint  
553 probabilistic weather forecasting from marginals. *arXiv preprint arXiv:2506.10772*, 2025.  
554555 Joshua J Alland, Brian H Tang, Kristen L Corbosiero, and George H Bryan. Combined effects  
556 of midlevel dry air and vertical wind shear on tropical cyclone development. part i: Downdraft  
557 ventilation. *Journal of the Atmospheric Sciences*, 78(3):763–782, 2021.558 American Meteorological Society. Tropical cyclone. Glossary of Meteorology, 2020. [http://glossary.ametsoc.org/wiki/Tropical\\_cyclone](http://glossary.ametsoc.org/wiki/Tropical_cyclone).  
559  
560561 Christian M Appendini. Developing rapid response protocols for rapidly intensifying tropical cyclones.  
562 *Bulletin of the American Meteorological Society*, 105(3):E518–E520, 2024.563 Alexander J. Baker, Benoît Vannière, and Pier Luigi Vidale. On the realism of tropical cyclone  
564 intensification in global storm-resolving climate models. *Geophysical Research Letters*, 51(17):  
565 e2024GL109841, 2024. doi: <https://doi.org/10.1029/2024GL109841>. URL <https://agupubs.onlinelibrary.wiley.com/doi/abs/10.1029/2024GL109841>. e2024GL109841  
566 2024GL109841.  
567568 E.A. Barnes, R.J. Barnes, and M. DeMaria. Sinh-arcsinh-normal distributions to add un- certainty to  
569 neural network regression tasks: Applications to tropical cyclone intensity forecasts. *Environmental  
570 Data Sci.*, 2:e15, 2023. doi: 0.1017/eds.2023.7.  
571572 Kaifeng Bi, Lingxi Xie, Hengheng Zhang, Xin Chen, Xiaotao Gu, and Qi Tian. Accurate medium-  
573 range global weather forecasting with 3D neural networks. *Nature*, 619(7970):533–538, 2023.  
574 ISSN 1476-4687. doi: 10.1038/s41586-023-06185-3.  
575576 Marja Bister and Kerry A Emanuel. Low frequency variability of tropical cyclone potential intensity  
577 1. interannual to interdecadal variability. *Journal of Geophysical Research: Atmospheres*, 107  
578 (D24):ACL–26, 2002.579 Boris Bonev, Thorsten Kurth, Christian Hundt, Jaideep Pathak, Maximilian Baust, Karthik Kashinath,  
580 and Anima Anandkumar. Spherical Fourier neural operators: Learning stable dynamics on the  
581 sphere, 2023. URL <http://arxiv.org/abs/2306.03838>.  
582583 P. Bougeault and Coauthors. The THORPEX interactive grand global ensemble. *Bull. Amer. Meteor.  
584 Soc.*, 91:1059–1072, 2010. doi: 10.1175/2010BAMS2853.1.  
585586 Stella Bourdin and Leo Saffin. Huracanpy: A python package for reading and analysing cyclone  
587 tracks. *Journal of Open Source Software*, 10(111):8174, 2025. doi: 10.21105/joss.08174. URL  
588 <https://doi.org/10.21105/joss.08174>.  
589590 Glenn W. Brier. Verification of forecasts expressed in terms of probability. *Monthly Weather Review*,  
591 78(1):1–3, 1950. doi: 10.1175/1520-0493(1950)078<0001:VOFEIT>2.0.CO;2.  
592593 William J. Broad. Artificial intelligence gives weather forecasters a new edge, July  
594 2024. URL <https://www.nytimes.com/interactive/2024/07/29/science/ai-weather-forecast-hurricane.html>. The New York Times, Published July 29,  
595 2024. Accessed May 14, 2025.

- 594 Tomer Burg and Sam Lillo. TroPYcal, 2019. URL <https://github.com/tropycal/tropycal>. Github repository.
- 595
- 596
- 597 J.P Cangialosi, E. Blake, M. DeMaria, A. Penny, A. Latto, E. Rappaport, and V. Tallapragada. Recent  
598 progress in tropical cyclone intensity forecasting at the National Hurricane Center. *Weather and  
599 Forecasting*, 35:1913–1922, 2020. doi: 10.1175/WAF-D-20-0059.1.
- 600 Daniel R Chavas, Ning Lin, and Kerry Emanuel. A model for the complete radial structure of the  
601 tropical cyclone wind field. part i: Comparison with observed structure. *Journal of the Atmospheric  
602 Sciences*, 72(9):3647–3662, 2015.
- 603
- 604 CA Davis. Resolving tropical cyclone intensity in models. *Geophysical Research Letters*, 45(4):  
605 2082–2087, 2018.
- 606 M. DeMaria and J. Kaplan. A statistical hurricane intensity prediction scheme (SHIPS) for the  
607 Atlantic basin. *Wea. Forecasting*, 9:209–220, 1994. doi: 10.1175/1520-0434(1994)009<0209:  
608 ASHIPS>2.0.CO;2.
- 609
- 610 M. DeMaria, C. R. Sampson, J. A. Knaff, and K. D. Musgrave. Is tropical cyclone intensity guidance  
611 improving? *Bull. Amer. Meteor. Soc.*, 95:387–398, 2014. doi: 10.1175/BAMS-D-12-00240.1.
- 612 M. DeMaria, J.L. Franklin, M.J. Onderlinde, and J. Kaplan. Operational forecasting of tropical  
613 cyclone rapid intensification at the National Hurricane Center. *Atmosphere*, 12:683, 2021. doi:  
614 10.3390/atmos12060683.
- 615
- 616 Mark DeMaria, Michelle Mainelli, Lynn K. Shay, John A. Knaff, and John Kaplan. Further improve-  
617 ments to the statistical hurricane intensity prediction scheme (ships). *Weather and Forecasting*, 20  
618 (4):531 – 543, 2005.
- 619 Mark DeMaria, James L. Franklin, Rachel Zelinsky, David A. Zelinsky, Matthew J. Onder-  
620 linde, John A. Knaff, Stephanie N. Stevenson, John Kaplan, Kate D. Musgrave, Galina  
621 Chirokova, and Charles R. Sampson. The national hurricane center tropical cyclone  
622 model guidance suite. *Weather and Forecasting*, 37(11):2141 – 2159, 2022. doi: 10.  
623 1175/WAF-D-22-0039.1. URL <https://journals.ametsoc.org/view/journals/wefo/37/11/WAF-D-22-0039.1.xml>.
- 624
- 625 Mark DeMaria, James L. Franklin, Galina Chirokova, Jacob Radford, Robert DeMaria, Kate D.  
626 Musgrave, and Imme Ebert-Uphoff. Evaluation of tropical cyclone track and intensity forecasts  
627 from artificial intelligence weather prediction (aiwp) models, 2024. URL <https://arxiv.org/abs/2409.06735>.
- 628
- 629 William Dulac, Julien Cattiaux, Fabrice Chauvin, Stella Bourdin, and Sébastien Fromang. Assessing  
630 the representation of tropical cyclones in era5 with the cnrm tracker. *Climate Dynamics*, 62(1):  
631 223–238, 2024.
- 632
- 633 Imme Ebert-Uphoff and Kyle Hilburn. The outlook for ai weather prediction, 2023.
- 634
- 635 Kerry A Emanuel. An air-sea interaction theory for tropical cyclones. part i: Steady-state maintenance.  
636 *Journal of Atmospheric Sciences*, 43(6):585–605, 1986.
- 637
- 638 Kerry A Emanuel. Thermodynamic control of hurricane intensity. *Nature*, 401(6754):665–669, 1999.
- 639 M.A. Fernandez, E.A. Barnes, R.J. Barnes, M. DeMaria, M. McGraw, G. Chirokova, and L. Lu.  
640 Predicting tropical cyclone track forecast errors using a probabilistic neural network. *Artificial  
641 Intelligence for the Earth Systems*, 4, 2025. doi: 10.1175/AIES-D-24-0066.1.
- 642
- 643 Jennifer Gahtan, Kenneth R. Knapp, Carl J. III Schreck, Howard J. Diamond, James P. Kossin, and  
644 Michael C. Kruk. International best track archive for climate stewardship (ibtracs) project, version  
645 4.01, 2024. URL <https://doi.org/10.25921/82ty-9e16>. [indicate subset used].
- 646
- 647 Saranya Ganesh Sudheesh, Tom Beucler, Frederick Iat-Hin Tam, Milton S. Gomez, Jakob Runge, and  
648 Andreas Gerhardus. Selecting robust features for machine-learning applications using multidata  
649 causal discovery. *Environmental Data Science*, 2:e27, 2023. doi: 10.1017/eds.2023.21.

- 648 Tilmann Gneiting and Adrian E Raftery and. Strictly proper scoring rules, prediction, and es-  
 649 timation. *Journal of the American Statistical Association*, 102(477):359–378, 2007. doi:  
 650 10.1198/016214506000001437.
- 651
- 652 Milton Gomez, Louis Poulaing-Auzéau, Alexis Berne, and Tom Beucler. Global forecasting of tropical  
 653 cyclone intensity using neural weather models. *arXiv preprint arXiv:2508.17903*, 2025.
- 654
- 655 S.M. Griffin, A. Wimmers, and C.S. Velden. Predicting rapid intensification in North Atlantic  
 656 and eastern North Pacific tropical cyclones using a convolutional neural network. *Weather and  
 Forecasting*, 37:1333–1355, 2022. doi: 10.1175/WAF-D-21-0194.1.
- 657
- 658 Danan Gu, Kirill Andreev, and Matthew E Dupre. Major trends in population growth around the  
 659 world. *China CDC weekly*, 3(28):604, 2021.
- 660
- 661 Andrew Hazelton, Ghassan J Alaka Jr, Lew Gramer, William Ramstrom, Sarah Ditche, Xiaomin  
 662 Chen, Bin Liu, Zhan Zhang, Lin Zhu, Weiguo Wang, et al. 2022 real-time hurricane forecasts from  
 663 an experimental version of the hurricane analysis and forecast system (hafsv0. 3s). *Frontiers in  
 Earth Science*, 11:1264969, 2023.
- 664
- 665 JT Heming. Tropical cyclone tracking and verification techniques for met office numerical weather  
 666 prediction models. *Meteorological Applications*, 24(1):1–8, 2017.
- 667
- 668 Hans Hersbach, Bill Bell, Paul Berrisford, Shoji Hirahara, András Horányi, Joaquín Muñoz-Sabater,  
 669 Julien Nicolas, Carole Peubey, Raluca Radu, Dinand Schepers, et al. The era5 global reanalysis.  
 670 *Quart. J. Roy. Meteorol. Soc.*, 146(730):1999–2049, 2020.
- 671
- 672 Cheng Huang, Cong Bai, Sixian Chan, Jinglin Zhang, and YuQuan Wu. Mgtcf: multi-generator  
 673 tropical cyclone forecasting with heterogeneous meteorological data. In *Proceedings of the AAAI  
 Conference on Artificial Intelligence*, volume 37, pp. 5096–5104, 2023.
- 674
- 675 Cheng Huang, Pan Mu, Jinglin Zhang, Sixian Chan, Shiqi Zhang, Hanting Yan, Shengyong Chen, and  
 676 Cong Bai. Benchmark dataset and deep learning method for global tropical cyclone forecasting.  
 677 *Nature Communications*, 16(1):5923, 2025.
- 678
- 679 J. Kaplan and M. DeMaria. An updated statistical hurricane intensity prediction scheme (SHIPS) for  
 the Atlantic and eastern North Pacific basins. *Weather and Forecasting*, 14:326–337, 1999.
- 680
- 681 J. Kaplan, M. DeMaria, and J.A. Knaff. A revised tropical cyclone rapid intensification index for the  
 682 Atlantic and eastern North Pacific basins. *Weather and Forecasting*, 25:220–241, 2010.
- 683
- 684 J. Kaplan, C.M. Rozoff, M. DeMaria, C.R. Sampson, J.P. Kossin, C.S. Velden, J.J. Cione, J.P. Dunion,  
 685 J.A. Knaff, J.A. Zhang, J.F. Dostalek, J.D. Hawkins, T.F. Lee, and J.E. Solbrig. Evaluating  
 686 environmental impacts on tropical cyclone rapid intensification. *Weather and Forecasting*, 30:  
 1374–1396, 2015. doi: 10.1175/WAF-D-15-0032.1.
- 687
- 688 John Kaplan and Mark DeMaria. Large-scale characteristics of rapidly intensifying  
 689 tropical cyclones in the north atlantic basin. *Weather and Forecasting*, 18(6):1093  
 – 1108, 2003. doi: 10.1175/1520-0434(2003)018<1093:LCORIT>2.0.CO;2. URL  
 690 [https://journals.ametsoc.org/view/journals/wefo/18/6/1520-0434\\_2003\\_018\\_1093\\_lcorit\\_2\\_0\\_co\\_2.xml](https://journals.ametsoc.org/view/journals/wefo/18/6/1520-0434_2003_018_1093_lcorit_2_0_co_2.xml).
- 691
- 692
- 693 J. A. Knaff, M. DeMaria, C. R. Sampson, and J. M. Gross. Statistical, 5-day tropical cyclone intensity  
 694 forecasts derived from climatology and persistence. *Wea. Forecasting*, 18:80–92, 2003. doi:  
 695 10.1175/1520-0434(2003)018<0080:SDTCIF>2.0.CO;2.
- 696
- 697 J.A. Knaff, C.R. Sampson, and K.D. Musgrave. An operational rapid intensification prediction  
 698 aid for the western North Pacific. *Weather and Forecasting*, 33:799–811, 2018. doi: 10.1175/  
 699 WAF-D-18-0012.1.
- 700
- 701 Kenneth R Knapp, Michael C Kruk, David H Levinson, Howard J Diamond, and Charles J Neumann.  
 The international best track archive for climate stewardship (ibtracs) unifying tropical cyclone data.  
*Bulletin of the American Meteorological Society*, 91(3):363–376, 2010.

- 702 T. Knutson. Global warming and hurricanes: An overview of current research results. Technical report,  
 703 Geophysical Fluid Dynamics Laboratory, National Oceanic and Atmospheric Administration, 2024.  
 704
- 705 Remi Lam, Alvaro Sanchez-Gonzalez, Matthew Willson, Peter Wirsberger, Meire Fortunato, Ferran  
 706 Alet, Suman Ravuri, Timo Ewalds, Zach Eaton-Rosen, Weihua Hu, Alexander Merose, Stephan  
 707 Hoyer, George Holland, Oriol Vinyals, Jacklynn Stott, Alexander Pritzel, Shakir Mohamed, and  
 708 Peter Battaglia. Learning skillful medium-range global weather forecasting, 2023.
- 709 Simon Lang, Mihai Alexe, Matthew Chantry, Jesper Dramsch, Florian Pinault, Baudouin Raoult,  
 710 Mariana CA Clare, Christian Lessig, Michael Maier-Gerber, Linus Magnusson, et al. Aifs–ecmwf’s  
 711 data-driven forecasting system. *arXiv preprint arXiv:2406.01465*, 2024.
- 712
- 713 Yi Li, Youmin Tang, Shuai Wang, Ralf Toumi, Xiangzhou Song, and Qiang Wang. Recent increases  
 714 in tropical cyclone rapid intensification events in global offshore regions. *Nature Communications*,  
 715 14(1):5167, 2023.
- 716 Joseph W Lockwood, Avantika Gori, and Pierre Gentine. A generative super-resolution model for  
 717 enhancing tropical cyclone wind field intensity and resolution. *Journal of Geophysical Research: Machine Learning and Computation*, 1(4):e2024JH000375, 2024a.
- 718
- 719 Joseph W Lockwood, Ning Lin, Avantika Gori, and Michael Oppenheimer. Increasing flood hazard  
 720 posed by tropical cyclone rapid intensification in a changing climate. *Geophysical Research Letters*,  
 721 51(5):e2023GL105624, 2024b.
- 722
- 723 A.E. Mercer, A.D. Grimes, and K.M. Wood. Application of unsupervised learning techniques to  
 724 identify Atlantic tropical cyclone rapid intensification environments. *J. App. Meteorol. and Climat.*,  
 725 60:119–138, 2021. doi: 10.1175/JAMC-D-20-0105.1.
- 726
- 727 Juan Nathaniel, Yongquan Qu, Tung Nguyen, Sungduk Yu, Julius Busecke, Aditya Grover,  
 728 and Pierre Gentine. Chaosbench: A multi-channel, physics-based benchmark for  
 729 subseasonal-to-seasonal climate prediction. In A. Globerson, L. Mackey, D. Belgrave,  
 730 A. Fan, U. Paquet, J. Tomczak, and C. Zhang (eds.), *Advances in Neural Information Processing Systems*, volume 37, pp. 43715–43729. Curran Associates, Inc., 2024.  
 731 URL [https://proceedings.neurips.cc/paper\\_files/paper/2024/file/4d3684dd7926754b48bc6cd99a840232-Paper-Datasets\\_and\\_Benchmarks\\_Track.pdf](https://proceedings.neurips.cc/paper_files/paper/2024/file/4d3684dd7926754b48bc6cd99a840232-Paper-Datasets_and_Benchmarks_Track.pdf).
- 732
- 733
- 734 Barbara Neumann, Athanasios T Vafeidis, Juliane Zimmermann, and Robert J Nicholls. Future  
 735 coastal population growth and exposure to sea-level rise and coastal flooding—a global assessment.  
 736 *PloS one*, 10(3):e0118571, 2015.
- 737
- 738 Alexander K Nickerson, Jun A Zhang, Robert H Weisberg, and Yonggang Liu. Rapid intensification  
 739 of hurricane ian (2022) in high shear. *Journal of Geophysical Research: Atmospheres*, 130(13):  
 740 e2024JD042024, 2025.
- 741
- 742 NOAA National Centers for Environmental Information. U.S. Billion-Dollar Weather and Climate  
 743 Disasters (2025). <https://www.ncei.noaa.gov/access/billions/>, 2025. Accessed: 09/05/2025.
- 744
- 745 Young-Jae Park, Minseok Seo, Doyi Kim, Hyeri Kim, Sanghoon Choi, Beomkyu Choi, Jeongwon  
 746 Ryu, Sohee Son, Hae-Gon Jeon, and Yeji Choi. Long-term typhoon trajectory prediction: A  
 747 physics-conditioned approach without reanalysis data. In *The Twelfth International Conference on Learning Representations*, 2023.
- 748
- 749 Jaideep Pathak, Shashank Subramanian, Peter Harrington, Sanjeev Raja, Ashesh Chattopadhyay,  
 750 Morteza Mardani, Thorsten Kurth, David Hall, Zongyi Li, Kamyar Azizzadenesheli, Pedram  
 751 Hassanzadeh, Karthik Kashinath, and Animashree Anandkumar. FourCastNet: A global data-  
 752 driven high-resolution weather model using adaptive fourier neural operators, 2022. URL <http://arxiv.org/abs/2202.11214>.
- 753
- 754 Henri Rossi Pinheiro, Kevin Ivan Hodges, and Manoel Alonso Gan. An intercomparison of subtropical  
 755 cut-off lows in the southern hemisphere using recent reanalyses: Era-interim, ncep-cfrs, merra-2,  
 jra-55, and jra-25. *Climate Dynamics*, 54(1):777–792, 2020.

- 756 Ilan Price, Alvaro Sanchez-Gonzalez, Ferran Alet, Tom R Andersson, Andrew El-Kadi, Dominic  
 757 Masters, Timo Ewalds, Jacklynn Stott, Shakir Mohamed, Peter Battaglia, et al. Probabilistic  
 758 weather forecasting with machine learning. *Nature*, 637(8044):84–90, 2025.
- 759
- 760 James F Price. Upper ocean response to a hurricane. *Journal of Physical Oceanography*, 11(2):  
 761 153–175, 1981.
- 762 Stephan Rasp. AI-Weather SotA vs Time. 12 2024. doi: 10.6084/m9.figshare.28083515.  
 763 v1. URL [https://figshare.com/articles/dataset/AI-Weather\\_SotA\\_vs\\_Time/28083515](https://figshare.com/articles/dataset/AI-Weather_SotA_vs_Time/28083515).
- 764
- 765 Stephan Rasp, Stephan Hoyer, Alexander Merose, Ian Langmore, Peter Battaglia, Tyler Russell,  
 766 Alvaro Sanchez-Gonzalez, Vivian Yang, Rob Carver, Shreya Agrawal, et al. Weatherbench 2: A  
 767 benchmark for the next generation of data-driven global weather models. *Journal of Advances in  
 768 Modeling Earth Systems*, 16(6):e2023MS004019, 2024.
- 769
- 770 Muhammad Naufal Razin, Christopher J. Slocum, John A. Knaff, Paula J. Brown, and Michael M.  
 771 Bell. Tropical cyclone precipitation, infrared, microwave, and environmental dataset (tc  
 772 primed). *Bulletin of the American Meteorological Society*, 104(11):E1980 – E1998, 2023.  
 773 doi: 10.1175/BAMS-D-21-0052.1. URL <https://journals.ametsoc.org/view/journals/bams/104/11/BAMS-D-21-0052.1.xml>.
- 774
- 775 C.M. Rozoff and J.P. Kossin. New probabilistic forecast models for the prediction of tropical cyclone  
 776 rapid intensification. *Weather and Forecasting*, 26:677–689, 2011. doi: 10.1175/WAF-D-10-05059.  
 777 1.
- 778
- 779 Pankaj Lal Sahu, Sukumaran Sandeep, and Hariprasad Kodamana. Evaluating global machine  
 780 learning models for tropical cyclone dynamics and thermodynamics. *Journal of Geophysical  
 781 Research: Machine Learning and Computation*, 2(2):e2025JH000594, 2025. doi: <https://doi.org/10.1029/2025JH000594>. URL <https://agupubs.onlinelibrary.wiley.com/doi/abs/10.1029/2025JH000594> e2025JH000594 2025JH000594.
- 782
- 783 C.R. Sampson, J.A. Knaff, C.J. Slocum, M.J. Onderlinde, A. Brammer, M. Frost, and B. Strahl.  
 784 Deterministic rapid intensity forecast guidance for the Joint Typhoon 2 Warning Center's Area of  
 785 Responsibility. *Weather and Forecasting*, 2023. doi: 10.1175/WAF-D-23-0084.1.
- 786
- 787 Carl J Schreck III, Kenneth R Knapp, and James P Kossin. The impact of best track discrepancies on  
 788 global tropical cyclone climatologies using ibtracs. *Monthly Weather Review*, 142(10):3881–3899,  
 789 2014.
- 790
- 791 H. Shaiba and M. Hahsler. Applying machine learning methods for predicting tropical cyclone rapid  
 792 intensification events. *Research Journal of Applied Sciences, Engineering and Technology*, 8:  
 793 638–651, 2016. doi: 10.19026/rjaset.13.3050.
- 794
- 795 Vivek Singh, Gaurav Tiwari, Amarendra Singh, Rajeeb Samanta, Atul Kumar Srivastava, Deew-  
 796 wan Singh Bisht, Ashish Routray, Sushil Kumar, Shivaji Singh Patel, and Abhishek Lodh. Tropical  
 797 cyclones across global basins: Dynamics, tracking algorithms, forecasting, and emerging scienti-  
 798 metric research trends. *Meteorological Applications*, 32(3):e70067, 2025.
- 799
- 800 C.J. Slocum. What can we learn from random forest in the context of the tropical cyclone rapid  
 801 intensification problem? 2nd NOAA Workshop on Leveraging AI in the Environmental Sciences,  
 802 2021. URL [https://www.star.nesdis.noaa.gov/star/documents/meetings/2020AI/presentations/202101/20210128\\_Slocum.pptx](https://www.star.nesdis.noaa.gov/star/documents/meetings/2020AI/presentations/202101/20210128_Slocum.pptx).
- 803
- 804 H. Su, L. Wu, J.H. Jiang, R. Pai, A. Liu, A.J. Zhai, P. Tavallali, and M. DeMaria. Applying satellite  
 805 observations of tropical cyclone internal structures to rapid intensification forecast with machine  
 806 learning. *Geophys. Res. Lett.*, 47:L089102, 2020. doi: 10.1029/2020GL089102.
- 807
- 808 R.D. Torn and M. DeMaria. Validation of ensemble-based probabilistic tropical cyclone intensity  
 809 change. *Atmosphere*, 12:373, 2021. doi: 10.3390/atmos12030373.

810 P. A. Ullrich, C. M. Zarzycki, E. E. McClenney, M. C. Pinheiro, A. M. Stansfield, and K. A.  
 811 Reed. Tempestextremes v2.1: a community framework for feature detection, tracking, and  
 812 analysis in large datasets. *Geoscientific Model Development*, 14(8):5023–5048, 2021. doi:  
 813 10.5194/gmd-14-5023-2021. URL <https://gmd.copernicus.org/articles/14/5023/2021/>.

815 Yuqing Wang and C-C Wu. Current understanding of tropical cyclone structure and intensity  
 816 changes—a review. *Meteorology and Atmospheric Physics*, 87(4):257–278, 2004.

818 Martin LM Wong and Johnny CL Chan. Tropical cyclone intensity in vertical wind shear. *Journal of  
 819 the atmospheric sciences*, 61(15):1859–1876, 2004.

820 Qidong Yang, Chia-Ying Lee, and Michael K. Tippett. A long short-term memory model for global  
 821 rapid intensification prediction. *Weather and Forecasting*, 35(4):1203 – 1220, 2020.

822 Qidong Yang, Chia-Ying Lee, Michael K Tippett, Daniel R Chavas, and Thomas R Knutson. Machine  
 823 learning-based hurricane wind reconstruction. *Weather and Forecasting*, 37(4):477–493, 2022.

825 Michaël Zamo and Philippe Naveau. Estimation of the continuous ranked probability score with  
 826 limited information and applications to ensemble weather forecasts. *Mathematical Geosciences*,  
 827 50(2):209–234, 2018.

## 829 APPENDICES

### 831 A ACCOUNTABILITY AND REPRODUCIBILITY

833 TCBench is released under the open-source GNU General Public License. Continued development,  
 834 including updates discussed in the limitations section, will be managed on the official TCBench  
 835 GitHub page. Maintenance includes community support, issue tracking, and ongoing curation of  
 836 benchmark content. All assets are hosted on GitHub and HuggingFace to ensure stability and  
 837 accessibility.

#### 839 Resources:

- 840 • **Dataset:** Available at *redacted for anonymity*
- 841 • **Model Checkpoints:** *redacted for anonymity*
- 842 • **Code:** *redacted for anonymity*
- 843 • **Documentation:** *redacted for anonymity*

845 An anonymized subset of the code and data has been prepared and uploaded to ProtonDrive:

846 <https://drive.proton.me/urls/SKT1FGC3KG#1IOFkFcL4xOU>

848 Please note that though any reference to usernames and paths that might be used to identify the  
 849 developers were removed, metadata scrubs were not conducted. We request that reviewers refrain  
 850 from viewing file metadata in case any identifying information be contained within.

#### 851 A.1 HUGGINGFACE REPOSITORY STRUCTURE

853 We organize the TCBench HuggingFace repository as follows:

- 855 • `texttt2023_IBTrACS.csv`: The subset of IBTrACS with the storms and timestamps that we use  
 856 to evaluate models.
- 857 • `matched_tracks/`: A collection of CSVs with the tracks we evaluate as baselines, including  
 858 AIFS, FourCastNetv2, Weatherlab FNv3, GenCast, Panguweather, TIGGE GEFS, and TIGGE  
 859 IFS.
- 860 • `neural_weather_models/`: Raw, global neural weather model outputs for up to 5 days  
 861 lead time, initialized at each timestamp associated with a storm in `2023_IBTrACS.csv` (i.e., the  
 862 ground truth).
- 863 • `postprocessing_models/`: Postprocessing model weights and the data required to run  
 them on the test set.

864 A.2 GITHUB REPOSITORY STRUCTURE  
865866 We organize the TCBench Github repository as follows:  
867

- 868 • `track_processing/`: The TempestExtremes routines needed to generate the tracks associated with the neural weather models, and the python routines that rely on HuracanPY to match the tracks found with TempestExtremes to the TCs in IBTrACS.
- 869 • `utils/`: Collection of utilities used to process IBTrACS data, to process neural weather model data for post-processing, and to calculate metrics on the tracks.
- 870 • `scriptnames.py`: various python scripts used to generate the track baseline predictions (e.g., `baselines.py`, `climatology_maker.py`, `compute_persistence.py`), to evaluate a set of tracks (e.g., `evaluate_tracks.py`)
- 871
- 872
- 873
- 874
- 875

876 B GETTING STARTED  
877

878 We provide a detailed description of how to prepare the necessary data, perform training, and  
879 benchmark your own model on our website. Please visit the following URL to see the guide: *redacted*  
880 for *anonymity*. We also ask that if you encounter any issues to please feel free to contact us or raise  
881 an issue on GitHub.  
882

883 A getting started notebook for the anonymized review was prepared and is available at:  
884 <https://drive.proton.me/urls/SKT1FGC3KG#1IOFkFcL4xOU>  
885 under the filename *Getting Started.ipynb*  
886

887 C TCBENCH DATA ORGANIZATION AND WORKFLOW  
888889 C.1 DATA SOURCES  
890

891 TCBench integrates multiple observational, reanalysis, forecast model, and AI-based data sources  
892 relevant to tropical cyclone (TC) analysis and prediction. Table S1 summarizes datasets currently  
893 included, and points to additional datasets of relevance.  
894

895 **Atmospheric Field Data:** We use atmospheric field data from a variety of sources, including:  
896

- 897 • Climate reanalysis and forecast datasets including ERA-5, TIGGE, IFS, and GFS.
- 898 • Outputs from AI models, including PanguWeather, FourcastNet, and the single member version  
899 of AIFS 1.0.
- 900

## 901 C.2 DATA WORKFLOW

902 The TCBench workflow standardizes diverse data sources into a common format for evaluation:  
903

- 904 1. Forecast and reanalysis fields are subset in space (storm-centered region) and time (forecast  
905 lead times) using storm initialization from IBTrACS.
- 906 2. Model-specific track outputs (e.g., TIGGE XML files, neural weather model forecasts in  
907 netCDF format) are converted into a uniform CSV format that includes the storm identifier  
908 (taken from IBTrACS), position, maximum sustained wind, and minimum sea-level pressure.
- 909 3. A `TCTrack` object is created for each storm, encapsulating observed and predicted values  
910 across time steps.
- 911 4. Gridded predictors (e.g., neural weather model forecasts) are stored as multidimensional  
912 arrays [samples, time, lat, lon, variables] for use in ML-based experiments.  
913
- 914

915 C.3 DATA PROCESSING  
916

917 Each dataset undergoes preprocessing to ensure comparability:

Data Source	Description	Website	Provided
<b>Reanalysis</b>			
ERA5	European Re-Analysis 5	<a href="https://cds.climate.copernicus.eu/datasets/reanalysis-era5-pressure-levels?tab=overview">https://cds.climate.copernicus.eu/datasets/reanalysis-era5-pressure-levels?tab=overview</a>	No
<b>Operational Analysis</b>			
HRES Analysis	ECMWF's archive of operational analysis, distributed through MARS	<a href="https://confluence.ecmwf.int/display/UDOC/MARS+content#MARScontent-Atmosphericmodels#Analysis:~:text=models-,Analysis">https://confluence.ecmwf.int/display/UDOC/MARS+content#MARScontent-Atmosphericmodels#Analysis:~:text=models-,Analysis</a>	No
<b>Ground Truth</b>			
IBTrACS	Best Track Archive	<a href="https://www.ncdc.noaa.gov/ibtracs/">https://www.ncdc.noaa.gov/ibtracs/</a>	Yes
Extended Best-Tracks	TC tracks with size	<a href="https://rammb2.cira.colostate.edu/research/tropical-cyclones/tc_extended_best_track_dataset/">https://rammb2.cira.colostate.edu/research/tropical-cyclones/tc_extended_best_track_dataset/</a>	No
TC PRIMED	ML Ready Benchmark dataset	<a href="https://rammb-data.cira.colostate.edu/tcprimed/">https://rammb-data.cira.colostate.edu/tcprimed/</a>	No
<b>Statistical Models</b>			
SHIPS	Statistical Hurricane Intensity Prediction Scheme (developmental dataset)	<a href="https://rammb2.cira.colostate.edu/research/tropical-cyclones/ships/development_data/">https://rammb2.cira.colostate.edu/research/tropical-cyclones/ships/development_data/</a>	No
<b>Models</b>			
NCEP GFS	Global Forecast System	<a href="https://www.nco.ncep.noaa.gov/pmb/products/gfs/">https://www.nco.ncep.noaa.gov/pmb/products/gfs/</a>	No
TIGGE GFS	NCEP GEFS ensemble model tracks dataset	<a href="https://rda.ucar.edu/datasets/d330003/dataaccess/#">https://rda.ucar.edu/datasets/d330003/dataaccess/#</a>	Yes <sup>†</sup>
TIGGE IFS	ECMWF IFS ensemble model tracks dataset	<a href="https://rda.ucar.edu/datasets/d330003/dataaccess/#">https://rda.ucar.edu/datasets/d330003/dataaccess/#</a>	Yes <sup>†</sup>
PanguWeather	AI global model outputs	<a href="https://github.com/198808xc/Pangu-Weather">https://github.com/198808xc/Pangu-Weather</a>	Yes
FourCastNet	AI model outputs	<a href="https://github.com/NVlabs/FourCastNet">https://github.com/NVlabs/FourCastNet</a>	No
FourCastNetv2	AI model outputs	<a href="https://github.com/NVIDIA/torch-harmonics">https://github.com/NVIDIA/torch-harmonics</a>	Yes
AIFS	AI global forecasting	<a href="https://arxiv.org/abs/2406.01465">https://arxiv.org/abs/2406.01465</a>	Yes

Table S1: Data Sources Summary. <sup>†</sup> non-gridded data only

- **TIGGE ensembles:** Extract ensemble mean and member tracks, harmonize to IBTrACS temporal resolution.
- **AI models:** Post-process global forecasts to storm-centered tracks; derive intensity and MSLP comparable to IBTrACS.
- **Post-processing Models:** Extract 50 member ensemble from parametric distribution through sampling, clip predictions to physical values ( $V_{max} \geq 0 \text{ kt}$ ).

Environmental Variable	Pressure Level (hPa)																	
	1000	975	950	925	900	850	800	700	600	500	400	300	250	200	150	100	50*	
Relative Vorticity	✓	✓	✓	✓	✓	✓	✓	✓	✓	✓	✓	✓	✓	✓	✓	✓	✓	
Relative Humidity	✓	✓	✓	✓	✓	✓	✓	✓	✓	✓	✓	✓	✓	✓	✓	✓	✓	
Geopotential Height	✓	✓	✓	✓	✓	✓	✓	✓	✓	✓	✓	✓	✓	✓	✓	✓	✓	
Vertical Velocity	✓	✓		✓		✓		✓	✓	✓	✓	✓	✓	✓	✓	✓	✓	
Horizontal Divergence	✓			✓		✓	✓	✓	✓	✓	✓	✓	✓	✓	✓	✓	✓	
Equivalent Potential Temperature	✓			✓		✓		✓	✓	✓	✓	✓	✓	✓	✓			
Zonal Wind (u)	✓			✓		✓		✓		✓		✓	✓	✓				
Meridional Wind (v)	✓			✓		✓		✓		✓		✓	✓	✓				

Table S2: Pressure level environmental fields potentially useful for TC intensity prediction. Adapted from (Ganesh Sudheesh et al., 2023).

Temperature (2m)	Dew point temperature (2m)
Convective available potential energy	Sea surface temperature
Total column water vapor	Total column cloud ice water
Total column cloud liquid water	Total column super-cooled liquid water
Total column cloud rain water	Vertical integral of divergence of cloud frozen water flux
Vertical integral of divergence of cloud liquid water flux	Vertical integral of divergence of mass flux
Vertical integral of divergence of moisture flux	Vertical integral of divergence of total energy flux
Vertical integral of potential and internal energy	

Table S3: Single level environmental fields potentially useful for TC intensity prediction. Adapted from (Ganesh Sudheesh et al., 2023).

#### C.4 MODEL EVALUATION AND METRICS

We evaluate forecast performance using the following metrics, standard in tropical cyclone verification:

- **Track error:** Great-circle distance (km) between forecast and observed positions.
- **Intensity error:** Mean absolute error (MAE) of maximum sustained winds (kt) and minimum sea-level pressure (hPa).
- **Skill scores:** Relative to climatology, persistence, and SHIPS baselines.
- **Probabilistic metrics:** Brier score and reliability diagrams for ensemble/AI probability forecasts.
- **Partitioning:** Cross-validation by year ensures temporal independence between training and evaluation sets.

#### C.5 BIASES AND LIMITATIONS

- The dataset represents a subset of all possible TC tracks; some regions and seasons may be underrepresented, especially where fewer storms materialize.

- Forecast evaluation may omit rare teleconnection patterns or unusual environmental scenarios, limiting generalizability.
- Definitions of storm intensity (e.g., 1-min vs. 10-min sustained winds) vary by agency and observation method, introducing potential inconsistencies across basins. We control for this by relying on USA reported values.
- IBTrACS quality varies by basin, with lower reliability in the South Indian Ocean and in the pre-satellite era.
- Reanalysis products such as ERA5 contain uncertainties in poorly observed regions and for weak or short-lived systems.
- AI models are rapidly updated (e.g., FourCastNet v1 vs. v2 vs. v3); benchmark results reflect the versions available to the authors at the time of dataset creation.
- Storm size and structural parameters are inconsistently available across sources, limiting evaluation beyond track and intensity.

## D BASELINE MODELS

TCBench provides a set of baseline models including traditional statistical approaches, numerical weather prediction (NWP) models, and simple machine learning (ML) approaches. These baselines serve as reference points for track, intensity, and rapid intensification forecasts.

### D.1 PERSISTENCE AND CLIMATOLOGY BASELINES

We rely on persistence and climatology as so called "naïve" baselines to provide context for the performance of the evaluated models against straightforward, transparent prediction methods.

- **Persistence:** Assumes that storm position, intensity, and structure remain unchanged from the current state. Provides a naive forecast useful for short-lead comparisons.
- **Climatology / Mean Track – Long Baseline (MT-LB):** Uses historical averages of storm positions and intensities within each basin and season to generate forecasts. Captures long-term trends and typical seasonal behavior.

### D.2 NUMERICAL WEATHER PREDICTION (NWP) BASELINES

We rely on physics-based Numerical Weather Prediction models as baselines for global predictions of TCs. These models rely on physics and numerical solutions of known equations to predict the state of the atmosphere based on initial conditions. We use the following models in TCBench:

- **NCEP GFS / GEFS:** Global Forecast System provides deterministic forecasts, while GEFS provides ensemble reforecasts from TIGGE. Baselines include position, maximum wind, and minimum sea-level pressure.
- **ECMWF IFS / TIGGE IFS:** Ensemble forecasts from ECMWF's Integrated Forecasting System. Used for both track and intensity benchmarks.

We take the data provided by TIGGE as it is openly available and due to computational limitations associated with running ensembles of physics-based NWP models.

### D.3 NEURAL WEATHER MODEL BASELINES

We rely on neural weather models available at the time of writing to provide baselines for global weather prediction using artificial intelligence. A brief description of the models is given below:

- **FourCastNetV2** - neural weather model that relies on spherical harmonics based neural operators to learn a grid-invariant evolution of the state of the atmosphere.
- **PanguWeather** - neural weather model that relies on an earth-specific transformer architecture and multiple, lead time specific models to predict the evolution of the atmosphere.
- **AIFS Single 1.0** - neural weather model whose architecture relies on a graph-based latent representation of the earth and a sliding window transformer processor in order to predict the

1080 evolution of the atmosphere.  
 1081 • **Weathernext Gen (GenCast)<sup>†</sup>** - neural weather model that relies on a conditional diffusion  
 1082 architecture to predict a possible evolution of the state of the atmosphere.  
 1083 • **FNv3<sup>†</sup>** - neural weather model that is not currently open, but is purported to be a functional  
 1084 generative network (FGN) (Alet et al., 2025) fine-tuned on IBTrACS to better predict tropical  
 1085 cyclones.  
 1086

1087 Track and intensity forecasts for the models marked with <sup>†</sup>are taken from Google WeatherLab  
 1088 (<https://deepmind.google.com/science/weatherlab>), due to either computational  
 1089 limitations for running the models or to the models not being open at the time of writing.  
 1090

#### 1091 D.4 POST PROCESSING BASELINES 1092

1093 We provide a set of postprocessing baseline models following Gomez et al. (2025). Each postprocess-  
 1094 ing model uses square, clipped neural weather model fields centered on the position of the tropical  
 1095 cyclone at the initial time of forecast, with an extent of +/- 30°latitude and longitude. These models  
 1096 further use an embedding of the position, maximum wind speed, and minimum sea level pressure at  
 1097 the initial time of forecast for their prediction. These models are set up for distributional regression of  
 1098 the rate of the intensification, and output the mean and standard deviation for a gaussian distribution  
 1099 associated with forecast. Of particular note, the postprocessing models only predict intensification,  
 1100 and do not predict the motion of the storm (i.e., the evolution of the position of the TC).  
 1101

1102 We provide three postprocessing models with varying levels of computational complexity:  
 1103

- 1104 • **Multiple Linear Regression:** the neural weather model forecasts are reduced (e.g., by calculat-  
 1105 ing extrema) and a pair of MLRs are trained to predict the mean and standard deviation of the rate  
 1106 of intensification.
- 1107 • **Multilayer Perceptron (ANN):** the neural weather model forecasts are reduced in a manner  
 1108 consistent with the reduction used for the MLR, but the regression algorithm is instead a MLP.
- 1109 • **UNet:** the neural weather model forecasts and an embedding of the scalar quantities associated  
 1110 with the forecast (e.g., the position and intensity at the initial time of forecast) are used in the  
 1111 regression task.

1112 We use the details provided for these architectures and associated hyperparameters provided by  
 1113 Gomez et al. (2025) in training the models.  
 1114

#### 1115 D.5 TRAINING SETUP 1116

1117 All baselines are trained and evaluated consistently:  
 1118

- 1119 • **Data Splits:** Storms are split into folds by year to minimize temporal leakage, ensuring that  
 1120 models are evaluated on unseen storms.
- 1121 • **Input Variables:** Depending on the baseline, inputs include:
  - 1124 – Current storm state: latitude, longitude, maximum wind, minimum pressure
  - 1125 – Environmental predictors: derived from ERA5 or TIGGE
  - 1126 – Historical storm statistics (for climatology/MT-LB)
- 1127 • **Ensemble Strategy:** For probabilistic evaluation, ML ensembles produce multiple real-  
 1129 izations; NWP ensembles (e.g., GEFS, IFS) are used directly as provided; Post-processing  
 1130 model output distributions are sampled to produce a 50-member ensemble.  
 1131

1132 Baseline forecasts are evaluated using the same deterministic, probabilistic, and rare event metrics  
 1133 described in Section 4.

1134  
1135 D.6 BASELINE MODELS SUMMARY TABLE  
1136

1137 Baseline	1138 Type	1139 Inputs	1140 Outputs / Target
Persistence	Deterministic	Current storm state	Track, intensity
Climatology / MT-LB	Statistical	Historical storm averages	Track, intensity
NCEP GFS / GEFS	NWP / Ensemble	Model initial conditions	Track, intensity
TIGGE IFS	NWP / Ensemble	Model initial conditions	Track, intensity
FourCastNetv2	AI	Model Initial Conditions	Track, intensity
PanguWeather	AI	Model Initial Conditions	Track, intensity
AIFS Single	AI	Model Initial Conditions	Track, intensity
WeatherNext Gen	AI	N/A <sup>*</sup>	Track, intensity
FNv3	AI	N/A <sup>*</sup>	Track, intensity
Pangu+MLR	PostProcessing AI	AI Model Forecasts, Current Storm state	Intensity
Pangu+ANN	PostProcessing AI	AI Model Forecasts, Current Storm state	Intensity
Pangu+UNet	PostProcessing AI	AI Model Forecasts, Current Storm state	Intensity

1151  
1152 Table 4: Summary of baseline models included in TCBench. Each baseline serves as a reference for  
1153 model evaluation.\*Forecasts taken directly from Google WeatherLab1154  
1155 E EVALUATION METRICS  
11561157  
1158 To test the forecast performance, TCBench use both deterministic and probabilistic metrics. De-  
1159 terministic evaluation focuses on the accuracy of predicted intensity and track positions. Standard  
1160 regression metrics include the root mean square error (RMSE), mean absolute error (MAE), and the  
1161 coefficient of determination ( $R^2$ ). Track errors are quantified using direct positional error (DPE),  
1162 cross-track error (CTE), and along-track error (ATE), which decompose the forecast position error  
1163 along and across the observed storm motion.1164  
1165 For probabilistic forecasts, we evaluate ensemble predictions using the Continuous Ranked Probability  
1166 Score (CRPS), which measures the discrepancy between the forecast distribution and the observed  
1167 outcome, capturing both ensemble accuracy and spread. For track forecasts, CRPS is generalized by  
1168 replacing absolute differences with Haversine distances between forecast and observed storm centers.  
1169 Additional probabilistic metrics include Brier Skill Score (BSS), Continuous ranked probability score  
1170 (CRPS), that provide complementary assessments of calibration and uncertainty representation. All  
1171 details of metrics and computational procedures for all metrics are provided in this section.1172 E.1 DETERMINISTIC METRICS  
1173

- 1174 • Root Mean Square Error (RMSE): Measures the square root of the average squared differ-  
1175 ences between predicted and actual values, indicating the model's prediction accuracy.
- 1176 • Mean Absolute Error (MAE): Represents the average absolute differences between predicted  
1177 and actual values, reflecting the magnitude of errors in predictions.
- 1178 • R-squared Score ( $R^2$ ): Quantifies the proportion of the variance in the dependent variable  
1179 that is predictable from the independent variables, indicating the model's explanatory power.

1180  
1181 **Direct Positional Error (DPE)** is the most basic measure of the positional accuracy of a tropical  
1182 cyclone (TC) forecast. It is defined as the distance between the forecast and observed positions of the  
1183 storm at the same *verification time (VT)*.1184  
1185 There are two commonly used approaches for calculating DPE:

- 1186
- 
- 1187 •
- Great Circle Distance (GCD)-based DPE:**
- This version computes the shortest distance
- 
- 1188 over the Earth's surface between the forecast and observed positions, treating Earth as a

1188 sphere. The *Haversine formula* is commonly used:  
 1189

$$1190 \quad d = 2r \arcsin \left( \sqrt{\sin^2 \left( \frac{\Delta\phi}{2} \right) + \cos(\phi_1) \cos(\phi_2) \sin^2 \left( \frac{\Delta\lambda}{2} \right)} \right)$$

$$1191 \quad 1192$$

1193 where:

- 1194 –  $\phi_1, \phi_2$  are the latitudes of the observed and forecast points (in radians),
- 1195 –  $\Delta\phi = \phi_2 - \phi_1$ ,  $\Delta\lambda = \lambda_2 - \lambda_1$  are the latitude and longitude differences,
- 1196 –  $r$  is the Earth's radius (typically  $\approx 6371$  km).

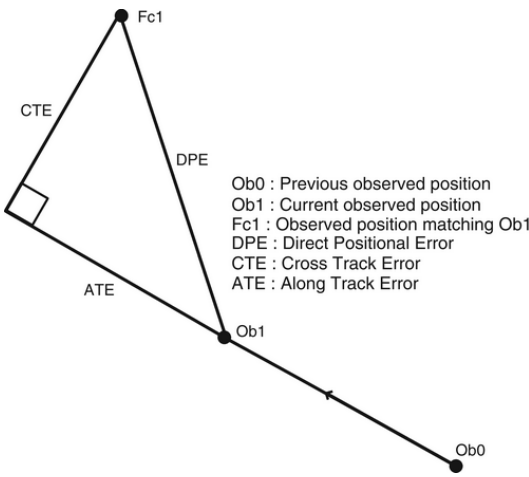
1197 This method accounts for Earth's curvature and is the standard in operational TC verification.

- 1198 • **Cartesian Projection-based DPE:** An alternative approach involves projecting both ob-  
 1199 served and forecast positions onto a local tangent plane (e.g., using an azimuthal equidistant  
 1200 or equirectangular projection). The DPE is then computed using standard Euclidean distance:
- 1201

$$1202 \quad d = \sqrt{(x_{\text{fcst}} - x_{\text{obs}})^2 + (y_{\text{fcst}} - y_{\text{obs}})^2}$$

1203 where  $(x, y)$  are the projected coordinates. This method may be preferred for regional  
 1204 studies or error decomposition in zonal/meridional directions.

1205 **Note:** DPE provides a scalar magnitude of error but does not convey directionality (e.g., north/south  
 1206 or ahead/behind). Directional errors are captured by the metrics below.



1207 Figure 5: Illustration of track error metrics adapted from (Heming, 2017)

1208 **Cross-Track Error (CTE)** measures the component of the track forecast error *perpendicular* to the  
 1209 observed direction of storm motion.

- 1210 1. Define the observed motion vector from the storm position 12 hours prior to VT to the  
 1211 observed position at VT.
  - 1212 2. Draw a perpendicular line from the forecast position to this vector.
  - 1213 3. Find the intersection point of this perpendicular with the observed vector.
  - 1214 4. CTE is the great circle distance between the forecast position and this intersection point.
- 1215 • In the **Northern Hemisphere**, a positive CTE indicates the forecast is to the **right** of the  
 1216 observed path.
  - 1217 • In the **Southern Hemisphere**, the interpretation is reversed.

1218 **Note:** CTE is undefined at the first valid time (due to lack of a 12-hour prior observed position).

1219 **Along-Track Error (ATE)** ATE measures the component of the error *along* the direction of storm  
 1220 motion and reflects timing accuracy.

- 1242 • Using the same intersection point from the CTE calculation, compute the great circle  
1243 distance between the observed position at VT and the intersection point.
- 1244
- 1245 • Positive ATE indicates the forecast is **ahead** of the observed position (i.e., storm is moving  
1246 too fast).
- 1247 • Negative ATE indicates the forecast is **behind** (i.e., storm is too slow).
- 1248

## 1249 E.2 PROBABILISTIC METRICS

1250 Here, we consider an ensemble of  $N$  forecasts as a set denoted  $\{x_i | i = 1, \dots, N\}$ , and  $\{x_i\}_N$  for  
1251 short.

1252 The **Brier skill score (BSS)** (Brier, 1950) is a relative measure that evaluates the improvement of a  
1253 probabilistic forecast over a reference forecast or climatology. BSS ranges  $-\infty$  to 1, where 1 indicates  
1254 a perfect skill and 0 indicates no improvement over the reference. A negative BSS suggests that the  
1255 forecast is less accurate than the reference. The BSS is based on the Brier Score (BS), a metric used  
1256 to measure the accuracy of probabilistic predictions for binary outcomes, defined as

$$1259 \text{BS} = \frac{1}{N} \sum_{i=1}^N (x_i - o_i)^2$$

1260 where  $x_i$  is a forecast probability,  $o_i$  is the actual outcome, and  $N$  is the number of forecasts. Then  
1261 BSS is defined as

$$1264 \text{BSS} = 1 - \frac{\text{BS}_{\text{forecast}}}{\text{BS}_{\text{reference}}}$$

1266 The **Continuous Ranked Probability Score (CRPS)** is widely used to assess the skill of ensemble  
1267 forecasts by measuring the discrepancy between the predicted and observed cumulative distribution  
1268 functions (CDFs). Unlike the BS, which applies to binary events, the CRPS evaluates the accuracy of  
1269 probabilistic forecasts for continuous variables. Formally, for a forecast CDF  $\hat{F}$  and a realized value  
1270  $y$ , the CRPS is

$$1271 \text{CRPS} = \int_{\mathbb{R}} \left[ \hat{F}(x) - \mathcal{H}(x - y) \right]^2 dx, \quad (2)$$

1273 where  $\mathcal{H}$  denotes the Heaviside step function, which represents the degenerate CDF of a single  
1274 observation. For discrete ensembles, we use the kernel representation of the CRPS (Gneiting & and,  
1275 2007):

$$1276 \text{CRPS}(\{x_i\}_N, y) = \frac{1}{N} \sum_{i=1}^N |x_i - y| - \frac{1}{2N^2} \sum_{i=1}^N \sum_{j=1}^N |x_i - x_j|. \quad (3)$$

1278 The first term is the mean absolute error of the ensemble members, while the second term measures  
1279 the ensemble spread via the mean absolute pairwise difference. To mitigate finite-ensemble bias  
1280 (inflated scores due to underestimation of the second term), we adopt the fair CRPS (Zamo & Naveau,  
1281 2018):

$$1282 \text{fCRPS}(\{x_i\}_N, y) = \frac{1}{N} \sum_{i=1}^N |x_i - y| - \frac{1}{2N(N-1)} \sum_{i=1}^N \sum_{j=1}^N |x_i - x_j|. \quad (4)$$

## 1285 E.3 METRICS FOR EXTREMES

1287 **Rapid Intensification:** Rapid intensification is a rare event, but not an exceedingly rare event; by  
1288 definition, it is the 95th percentile of intensity change. Thus, we evaluate model performance on rapid  
1289 intensification forecasts using metrics more tailored for rare event forecasts. We note that while most  
1290 of TCBench is configured as a **regression** problem, we have formulated rapid intensification as a  
1291 **binary classification problem**. This means rapid intensification models will be tasked with making  
1292 a simple “yes/no” prediction for the occurrence of rapid intensification.

- 1294 • Critical Success Index (CSI): Also known as the Threat Score, measures the ratio of correctly  
1295 predicted positive observations to the sum of all predicted positives, actual positives, and  
minus true positives. Can be used both for probabilistic track evaluation and RI.

- 1296  
 1297  
 1298  
 1299  
 1300
- Peirce skill score (PSS): The Peirce skill score (also known as the Hansen and Kuipers discriminant, or the true skill statistic) is an estimate of how well the forecast separates "yes" events from "no" events. It ranges from -1 to 1, with +1 being a perfect score and 0 indicating no skill. PSS is generally considered to be better for rare events, though for extremely rare events it tends to 0.

1301  
 1302 
$$\text{PSS} = \text{TPR} - \text{FPR} \quad \text{where } \text{TPR} = \frac{\text{TP}}{\text{TP} + \text{FN}}, \quad \text{FPR} = \frac{\text{FP}}{\text{FP} + \text{TN}}. \quad (5)$$
  
 1303

1304 **F EXTENDED RESULTS**  
 1305

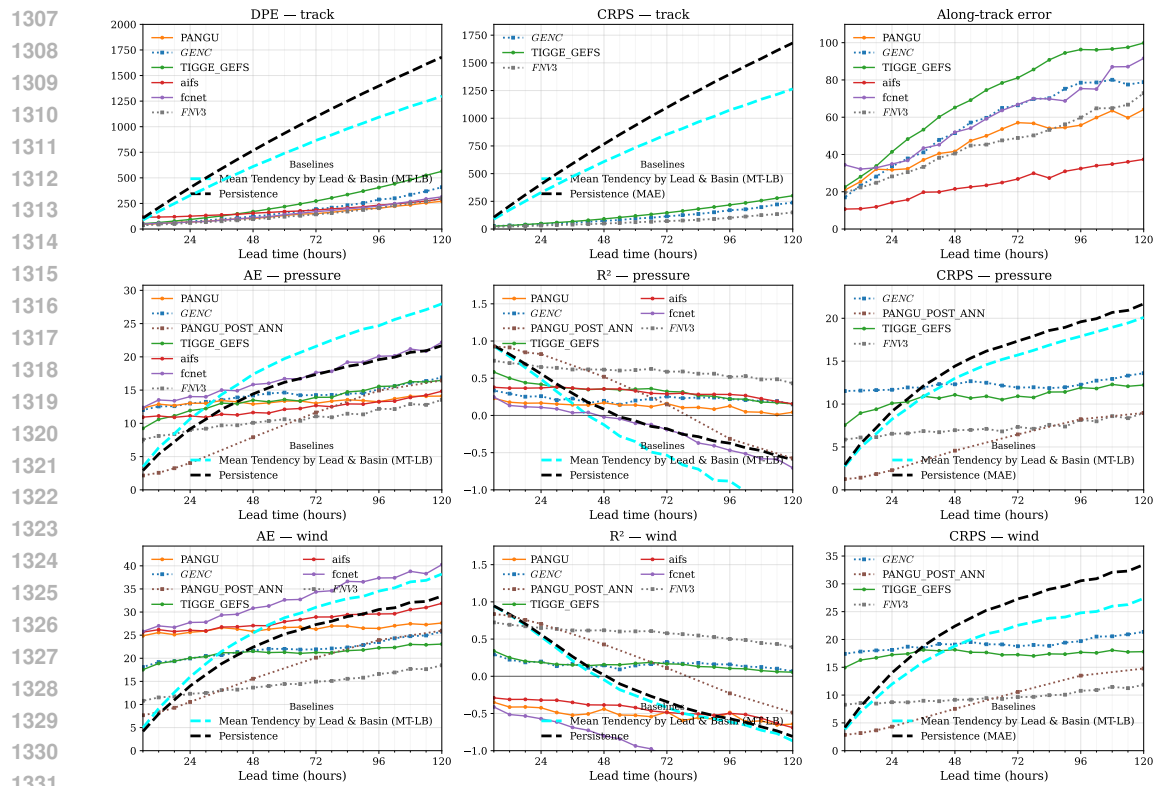


Figure 6: **Per-lead verification on TCbench-2023 (6–120 h), non-filled.** Rows: track, pressure, wind; columns: AE,  $R^2$ , CRPS (track uses DPE, CRPS-track, along-track). Curves use *raw model coverage*—no persistence filling—so each mean is over the forecast–verification pairs available for that model and lead. Models are colored (WeatherLab FNV3 in gray). Baselines: persistence (black dashed) and climatology/MT-LB (cyan dashed).  $R^2 = 1 - \text{MSE}/\text{Var}$  vs. IBTrACS

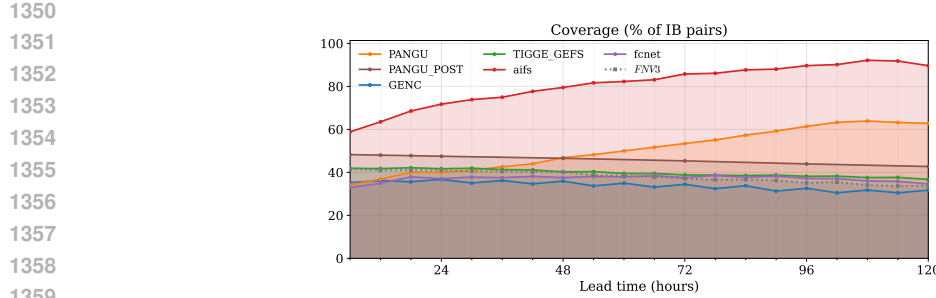


Figure 7: **Coverage on the 2023 test set (% of IBTrACS verification pairs) by lead.** An IBTrACS pair is a unique  $(\text{SID}, t_0, t_0+L)$  observed on the 6-hour grid with  $t_0 \in \{00, 12\}$  UTC. A model *covers* a pair if it outputs any row for that key. Shaded regions indicate the fraction covered at each lead. Large coverage disparities motivate the FAIR comparison (persistence-filled on the same IB grid) reported elsewhere in the paper.

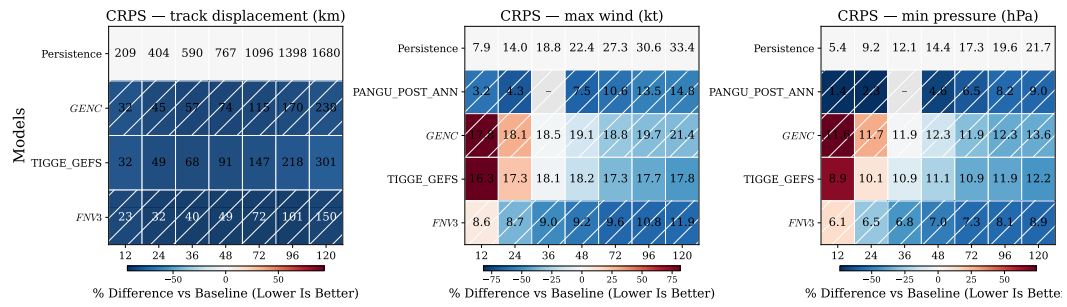


Figure 8: **CRPS scorecards (probabilistic).** Track displacement (km), max wind (kt), and min pressure (hPa) on TCbench-2023 for 6–120,h leads. Each cell is the percent difference in CRPS relative to the Persistence baseline at the same lead (lower is better); the Persistence row reports absolute CRPS (units in panel titles). Results use *non-filled* data (raw model coverage); dashes denote no verification pairs at that lead. Hatched rows mark externally provided products (GENC, FNv3); PANGU\_POST\_ANN is a learned post-processor.

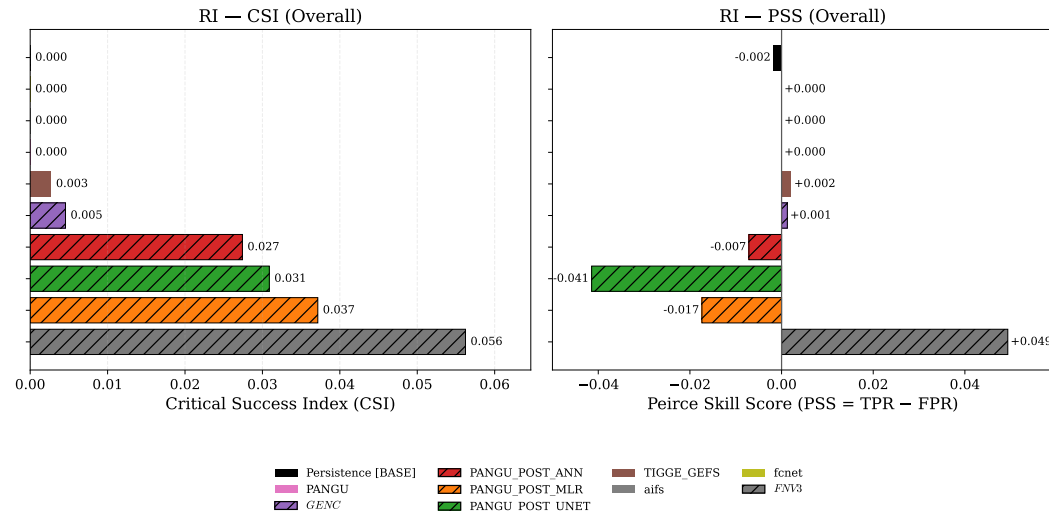


Figure 9: **Rapid Intensification (RI) skill—overall by model.** Bars show overall Critical Success Index (CSI; left) and Peirce Skill Score (PSS = TPR – FPR; right) computed against the IBTrACS RI ground truth for 2023. Scores use the common  $(\text{SID}, t_0, t_0+L)$  key set on the 6 h IBTrACS grid.

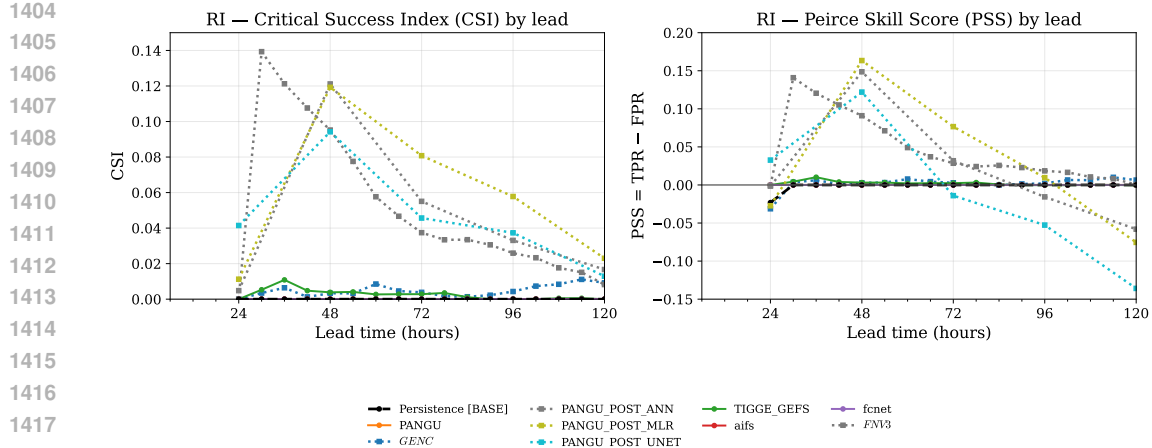


Figure 10: **Rapid Intensification (RI) skill by lead time.** CSI (left) and PSS (right) as a function of lead time (6–120 h, 6 h steps), evaluated vs. the IBTrACS 2023 RI ground truth on the 6 h grid. Axes are capped for readability.

## G POTENTIAL APPLICATIONS

Accurate assessments of the wind-related risks posed by tropical cyclones rely heavily on knowledge of their full wind structures (2D images stacked in the vertical). It is challenging to obtain such wind fields because satellite observations often only provide partial coverage of TCs with limited temporal sampling. Various methods have been proposed to address this challenge, ranging from analytical parametric models (Chavas et al., 2015) to modern machine learning techniques (Yang et al., 2022), which attempt to infer spatial wind fields from easily observed scalar quantities such as minimum sea-level pressure or the radius of maximum surface winds. By offering IBTrACS in an AI-ready format, TCBench facilitates the design and training of models to **predict key scalars needed for wind reconstruction**. Moreover, the standardized aggregation of outputs from multiple AI models allows users to assess and compare tropical cyclone size predictions across models, thereby helping to identify and quantify TC size biases in neural weather models.

By providing different routines to process TC observations in different formats, the TCBench dataset is ideal for **developing very short-term TC winds and precipitation predictions**. Data-driven nowcasting models (Agrawal et al., 2019) are more computationally competitive than explicitly simulating the TCs with high-resolution numerical models. The ability of probabilistic data-driven models to create hundreds of possible predictions for a given initial condition within minutes and adjust based on new satellite image inputs makes them useful additions to the existing weather forecasting pipeline.

The examples provided in the previous sections only evaluate the intensity at a given point in the TCs. Similar to the wind field reconstruction tasks described earlier, we can **develop wind downscaling models** (Lockwood et al., 2024a) to add additional spatial details to the TCs in the neural weather model outputs in coarse resolution. Another extension to the prediction tasks shown in the text is to provide **global prediction of TC activity across timescales**. The neural weather model outputs and simple tracking algorithm in TCBench facilitate consistent evaluation of the skill of different AI models in developing the TCs at the right time and right place. Based on the comparison of TC activity patterns of different neural weather models, basin-specific refinements can be made to reduce potential spatial biases in the existing trained neural weather models.

Finally, the aggregation of satellite images, environmental fields, and intensity observations in an easy-to-access dataset enables **identification of critical predictive environmental properties for TC intensity** (Bister & Emanuel, 2002), thereby forming the basis for novel discovery on tropical cyclone physics.

## 1458 H LIMITATIONS

---

1460 First, uncertainties associated with each product vary, which pose a challenge in estimating and  
1461 providing accurate error margins for reanalyses and observations. An ambitious goal is to include ob-  
1462 servational error estimates (e.g., intensity, track location) that vary over time, reflecting improvements  
1463 in satellites and technology.

1464 Although using multiple reanalyses and tracking algorithms is ideal due to the variation in data  
1465 quality and sensitivity of cyclone detection schemes, initial efforts may need to rely on a single  
1466 reanalysis dataset for tractability, while clearly acknowledging its limitations (Pinheiro et al., 2020).  
1467 Furthermore, creating a single dataset that fits all purposes is impossible, necessitating trade-offs  
1468 such as neglecting some teleconnections or using datasets only available for the past approximately  
1469 15 years. Additionally, the definition of TC intensity varies by agency, primarily in the number of  
1470 minutes used to calculate maximum sustained wind speeds, which introduces inconsistency.

1471 The first position of TCs across agencies and across time is also subject to large uncertainty and  
1472 inconsistency. Therefore, in subseasonal to seasonal time-scales and climate studies, it is common  
1473 to consider the first time the TC reaches tropical storm intensity (35 kt) in the track to improve  
1474 consistency. Moreover, creating a seamless list of predictors for the entire tropics is challenging due  
1475 to the variation in relevant variables across different basins or seasons.

1476

1477

1478

1479

1480

1481

1482

1483

1484

1485

1486

1487

1488

1489

1490

1491

1492

1493

1494

1495

1496

1497

1498

1499

1500

1501

1502

1503

1504

1505

1506

1507

1508

1509

1510

1511